Proc. Indian Acad. Sci. (Chem. Sci.), Vol. 94, No. 1, March 1985, pp. 201–240.

Particle motion in glasses

K J RAO and R PARTHASARATHY

Solid State and Structural Chemistry Unit, Indian Institute of Science, Bangalore 560012, India

1. Introduction

Glasses are a sub-group of amorphous materials obtained by the quenching of melts and may be distinguished from other non-crystalline materials by the fact that they exhibit the so-called 'glass transition' (Materials Advisory Board 1968). Glasses may be formed from practically all kinds of materials in which the strength of interparticle potentials range from very weak van der Waals (Bondi 1968) through metallic (Cahn 1980) and long range and non-directional ionic (Rao 1980, 1982) to the strongly directional covalent type (Rawson 1967). The stabilities of glasses so formed also vary widely: metallic glasses, for example, are prone to crystallize even before they undergo the glass transition (Angell 1981), while the so-called 'covalent network' glasses, such as B_2O_3 and SiO_2, are extremely resistant to devitrification (Rawson 1967).

It is well known that glasses retain an imprint of the parent liquid state and hence possess only short range order. The degree of such order, however, varies widely. Recent investigations, particularly those using high resolution electron microscopy (Gaskell *et al* 1979; Bursill *et al* 1981), have suggested the presence of well defined correlations over 50Å regions that could constitute the 'clusters' which characterize the mosaic of a glass. Evidently the particles (throughout this article we understand by the term 'particle', an atom, ion or molecule that is a sufficiently ultimate constituent of a glass) in a glass do not interact with identical potentials and therefore it should be appropriate to describe properties associated with such particles through the use of suitable distribution functions that reflect the distribution of such environments as quantitatively as possible.

The glass transition which marks the ultimate solidification of a supercooled melt is a complex phenomenon that has not been completely understood so far (Rao 1979; Cohen and Grest 1980). The super-cooled melt itself is in metastable equilibrium and a 'real-time' glass transition is a consequence of the system freezing out of this metastable equilibrium. A real glass, consequently, incorporates an excess free energy that manifests itself in a host of relaxation phenomena around the glass transition. The distribution of environments is characterized by a corresponding distribution of the excess free energy, and several irreversible phenomena and responses of glasses to external stimuli may possibly be traced to it. Broadly, all responses that characterize the return to equilibrium of a system perturbed by external stimuli such as alternating electrical or mechanical fields, electromagnetic radiation etc., may be described as 'relaxation phenomena' (Wong and Angell 1976). Information about particle motion in glasses can be extracted from a study of relaxations. It is the purpose of this article to briefly review the present understanding of different types of relaxation phenomena in

glasses which are characterized by different interaction potentials. In §2 we summarize the methods of investigating particle motions through the use of dielectric and mechanical relaxations, vibrational band shapes, spin resonance absorption relaxations and Mossbauer spectroscopy. In §3 we present some selected studies of glasses using these techniques which have some definitive or novel information related to particle motions. In §4 a rather brief summary of the results of computer experiments bearing on particle motions related to glasses is given and in §5 we present a summary of the conclusions.

2. Methods of studying particle motions

2.1 *Dielectric relaxation*

Very generally, the dielectric constant ε^* is a complex quantity and may be written $\varepsilon^* = \varepsilon' + i\varepsilon''$ (Daniel 1967; Owen 1963). The measured dielectric constant $\varepsilon(\omega) = |\varepsilon^*(\omega)|$, at frequency ω, may then be written, $\varepsilon(\omega) = [(\varepsilon')^2 + (\varepsilon'')^2]^{\frac{1}{2}}$. The complex nature of $\varepsilon^*(\omega)$ implies that the displacement current and applied field are out of phase by an angle δ such that $\varepsilon' = \varepsilon_s \cos\delta$ and $\varepsilon'' = \varepsilon_s \sin\delta$ (Daniel 1967; Owen 1963; Stevels 1977), where ε_s is the static dielectric constant, and

$$\tan\delta = \varepsilon''/\varepsilon'. \tag{1}$$

$\tan\delta$ is referred to as the loss tangent or dissipation factor. The term 'loss' implies that the out-of-phase component of the dielectric current which leads to power dissipation is proportional to $\sin\delta$ which for small δ is equal to $\tan\delta$ itself. The dependence of $\varepsilon^*(\omega)$ on frequency ω can easily be shown to be (Daniel 1967)

$$\varepsilon^*(\omega) = \varepsilon_\infty + (\varepsilon_s - \varepsilon_\infty)/(1 + i\omega\tau), \tag{2}$$

where ε_∞ is the high frequency limit of the dielectric constant. τ in (2) is the relaxation time whose significance is clearly seen in figure 1. Equation (2) implies that (Daniel 1967; Owen 1963)

$$\varepsilon' = \varepsilon_\infty + (\varepsilon_s - \varepsilon_\infty)/(1 + \omega^2\tau^2) \tag{3}$$

$$\varepsilon'' = (\varepsilon_s - \varepsilon_\infty)\omega\tau/(1 + \omega^2\tau^2) \tag{4}$$

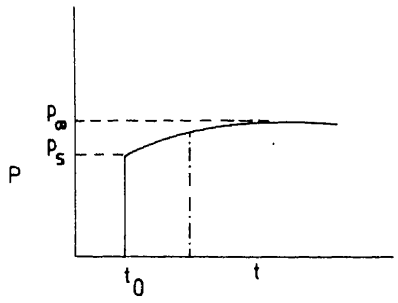

Figure 1. Time dependence of polarisation on applying a static field at t_0. The relaxation time, τ, is indicated by the line (– · – · –) where $P(\tau) = P_s + (P_\infty - P_s)(1 - 1/e)$.

whereupon tan δ may be written

$$\tan \delta = \varepsilon''/\varepsilon' = (\varepsilon_s - \varepsilon_\infty)\omega\tau/(\varepsilon_s + \varepsilon_\infty \omega^2 \tau^2). \tag{5}$$

Equations (2) to (5) are known as the Debye equations and assume the presence of a single relaxation time τ. The variation of ε' and ε'' as a function of $\omega\tau$ is shown in figure 2. An inspection of the above equations or of the figure suggests that ε'' and hence, tan δ, attains a maximum value when $\omega\tau = 1$ *i.e.* when $\omega_{max} = \tau^{-1}$. Similarly, it can be shown that (Owen 1963)

$$\varepsilon''_{max} = (\varepsilon_s - \varepsilon_\infty)/2 \tag{6}$$

$$\varepsilon'_{mid} = (\varepsilon_s + \varepsilon_\infty)/2 \tag{7}$$

$$\tan \delta_{max} = (\varepsilon_s - \varepsilon_\infty)/(\varepsilon_s + \varepsilon_\infty). \tag{8}$$

The full-width at half-maximum (FWHM) of the loss peak is roughly about 1·41 decades of frequency. The frequency corresponding to a maximum in tan δ, $\omega_{\tan \delta_{max}}$ is given by (Owen 1963)

$$\omega_{\tan \delta_{max}} = (\varepsilon_s/\varepsilon_\infty)^{\frac{1}{2}} \tau.$$

In general, however, the concept of a single relaxation time is an over-simplification, particularly for glasses, and the assumption of a distribution of relaxation times is more appropriate (Wong and Angell 1976; Owen 1963). A relaxation time spectrum may be represented by $G(\tau)$ such that $\int_0^\infty G(\tau)\,d\tau = 1$ (Owen 1963). The Debye equations (2–5) get modified appropriately and ε^* may then be written as (Owen 1963)

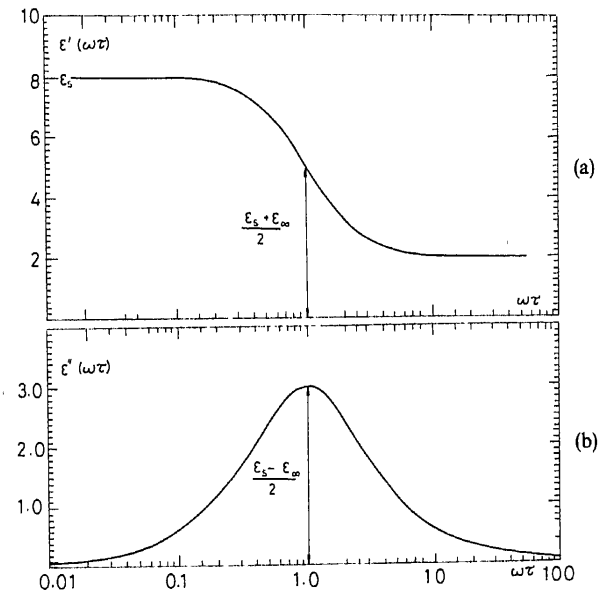

Figure 2. (**a**) The real part of ε^* as a function of log $\omega\tau$ for a dielectric with a single relaxation time. $\varepsilon_s = 8$, $\varepsilon_\infty = 2$; (**b**) the imaginary part of ε^* for the same dielectric (after Daniel 1967).

$$\varepsilon^* = \varepsilon_\infty + \left[(\varepsilon_s - \varepsilon_\infty) \int G(\tau)\,d\tau \right] \Big/ (1 + i\omega\tau). \tag{9}$$

Many types of distribution functions have been used; historically the oldest corresponds to a Gaussian probability function (Wagner 1913; Owen 1963) where

$$G(\tau)\,d\tau = (b/\pi)^{\frac{1}{2}} \exp(-b^2 z^2). \tag{10}$$

In this equation b is a constant and z corresponds to $\ln(\tau/\tau_0)$ where τ_0 is the peak value of the relaxation time. It is implicit in the use of a Gaussian that the intrinsic relaxation time τ_0 is broadened by an infinite number of independent causes. The breadth of the distribution increases rapidly as b decreases below 1. The introduction of a relaxation time distribution does not, however, materially alter ω_{max} which still corresponds to $(\tau_0)^{-1}$ and the total dispersion in ε' remains equal to $(\varepsilon_s - \varepsilon_\infty)/2$ (Owen 1963). Fuoss and Kirkwood (1941) have considered the possibility of deriving distribution functions based on experimental ε'' *vs* ω plots using transformation methods. Cole and Cole (1941) obtained a distribution function based on an empirical modification of the complex form of the Debye equation

$$\varepsilon^* = (\varepsilon_s - \varepsilon_\infty)/[1 + (i\omega\tau_0)^{1-\alpha}] \tag{11}$$

where α, $0 \leqslant \alpha \leqslant 1$, is a constant related to the width of the distribution. Another distribution function of an empirical origin that has been used to analyse asymmetric Cole–Cole plots (see later) is the Davidson–Cole function (Davidson and Cole 1951). It is yet another modification of the Debye equation and is written

$$\varepsilon^* - \varepsilon_\infty = (\varepsilon_s - \varepsilon_\infty)/(1 + i\omega\tau_0)^\beta \tag{12}$$

where β, $0 \leqslant \beta \leqslant 1$ is a constant similar to α.

The origin of the distribution functions has been discussed by many authors notable of whom are Kauzmann (1942) and Frohlich (1958). Kauzmann (1942) has applied the theory of chemical rate processes to the problem of dielectric relaxation times. In this approach the distribution of relaxation times originate from thermal fluctuations that cause changes in the environments of the relaxing dipoles (Owen 1963). As a consequence of such changes, a symmetric distribution of barriers results about the barrier height corresponding to the unperturbed state. Frohlich's (1958) analysis is more relevant to glasses in that it recognises the presence of a distribution of site symmetries and dipole environments in a glass. This very naturally leads to a relaxation time spectrum since $\tau_0 = \tau_0' \exp(-\Delta H/kT)$. A distribution in ΔH, therefore, may be regarded as the origin of the relaxation time spectrum in this approach. An advantage in Frohlich's approach is that irrespective of the initial distribution in ΔH, an increase in temperature should lead to narrowing of the relaxation time spectrum. This, of course, implies either that τ_0' is unaffected or that ΔH and $\ln \tau_0'$ vary proportionately, a feature verified in a number of systems.

Dielectric data is often represented using the Cole–Cole plot which is simply an Argand diagram (or a complex plane representation) of the real and imaginary components of ε^* (Cole and Cole 1941; Daniel 1967; Owen 1963). In the simple case of a Debye dielectric, the Cole–Cole plot (figure 3a) is a simple semi-circle terminated at ε_∞ and ε_s on the real axis (Daniel 1967; Owen 1963). The semi-circle itself is the locus of ε^* values each for a given value of $\omega\tau_0$. ε''_{max} corresponds to $\omega\tau_0 = 1$ and the equation of

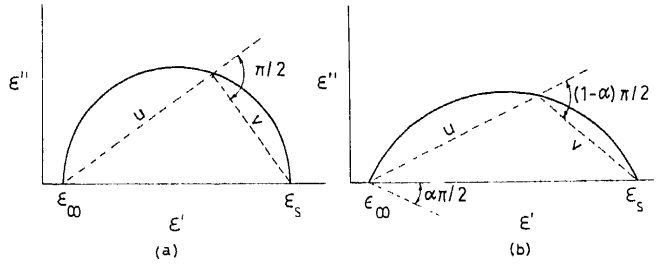

Figure 3. The Cole–Cole representations for (**a**) the Debye dielectric and (**b**) for a dielectric with a distribution of relaxation times (after Owen 1963).

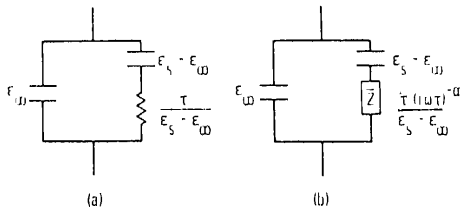

Figure 4. Equivalent circuit representations of (**a**) a Debye dielectric and (**b**) a dielectric with a distribution of relaxation times (after Owen 1963).

the semi-circle may be obtained by combining the Debye equations (Daniel 1967)

$$[\varepsilon' - (\varepsilon_\infty + \varepsilon_s)]^2/2 + (\varepsilon'')^2 = (\varepsilon_s - \varepsilon_\infty)^2/4. \tag{13}$$

Now, considering any two vectors **u** and **v** within the semi-circle one sees that the two are necessarily perpendicular to each other. The following equations may also be easily derived (Daniel 1967)

$$\mathbf{u} - \mathbf{v} = (\varepsilon_s - \varepsilon_\infty) \tag{14a}$$

and

$$\mathbf{u} = \varepsilon' - \varepsilon_\infty + i\varepsilon'' \tag{14b}$$

Using the definition of ε' (equation (3)) it is clear that

$$\mathbf{v} = \mathbf{u}i\omega\tau \tag{14c}$$

The generalized Cole–Cole distribution which takes into account the existence of a distribution of relaxation times simply amounts to modifying (14c) as (Daniel 1967)

$$\mathbf{v} = \mathbf{u}(i\omega\tau_0)^{1-\alpha} \tag{15}$$

The Cole–Cole plot for such a distribution is shown in figure 3b. It is the arc of a circle whose centre lies below the ε' axis and the line joining the centre of the semi-circle and ε_∞ makes an angle of $\alpha\pi/2$ with the ε' axis (Lovell *et al* 1976; Owen 1963).

Dielectric dispersion and relaxation are often conveniently understood using equivalent electrical circuits. Such circuits are shown in figure 4a for a Debye dielectric whose relaxation behaviour is depicted in figure 3a and in figure 4b for the Cole–Cole type of dielectric whose relaxation behaviour is shown in figure 3b. The capacitor ε_∞

gets charged instantaneously while the charging of $(\varepsilon_s - \varepsilon_\infty)$ may be regarded as being prevented by a resistance equal to $\tau/(\varepsilon_s - \varepsilon_\infty)$. In figure 4b the impedance corresponds to $\tau(i\omega\tau)^{-\alpha}/(\varepsilon_s - \varepsilon_\infty)$.

2.2 *Mechanical relaxation*

The response of a glass to cyclic mechanical stress may also be treated similarly (Litovitz and Davis 1965; Philipoff 1965). It is however, conventional to treat the behaviour of the modulus rather than the compressibility and this may be regarded as being equivalent to the dielectric constant. For the propagation of a shear wave in a viscoelastic medium, the shear modulus G^* may be written as (Wong and Angell 1976; Litovitz and Davis 1965)

$$G^* = G' + iG'' = G' + i\omega\eta_s \tag{16}$$

where ω is the angular frequency and η_s is the shear viscosity. When the static shear modulus is zero (as relevant to a glass above glass transition)

$$G' = G_\infty \omega^2 \tau_s^2/(1+\omega^2\tau_s^2) \tag{17}$$

and

$$G'' = G_\infty \omega\tau_s/(1+\omega^2\tau_s^2) = \omega\eta_s. \tag{18}$$

At low frequencies, $\eta_s = G_\infty \tau_s$. In mechanical relaxation studies it is often convenient to define a complex longitudinal modulus $M^* = M' + iM'' = K^* + 4G^*/3$ where K^* is the bulk modulus and G^* is the shear modulus. Litovitz and Davis (1965) have shown that M' and M'' may be approximated as

$$M' = \rho v^2 \quad \text{and} \quad M'' = 2\rho v^3/\alpha\omega \tag{19}$$

where α is the absorption coefficient and ρ and v are the density of the material and the velocity of sound, respectively. The absorption coefficient, α, may also be related to η using (Litovitz and Davis 1965)

$$\alpha\lambda = \pi\omega[(\eta_v + 4\eta_s/3)]/K_0 \tag{20}$$

where K_0 is the low frequency ('static') bulk modulus, η_v is the volume viscosity and λ the wave length of the ultrasonic wave. It is common in ultrasonic studies to relate the various moduli to acoustic impedances. The complex shear impedance, Z_s, for instance, may be written, (Litovitz and Davis 1965)

$$Z_s = \rho v_c = \rho[(1/v_s) + (\alpha/i\omega)]^{-1} = R_x + iX_s \tag{21}$$

using this, G' and G'' may be expressed as (Litovitz and Davis 1965)

$$G' = (R_s^2 - X_s^2)/\rho \tag{22a}$$

and

$$G'' = 2R_sX_s/\rho. \tag{22b}$$

Since an applied mechanical disturbance propagates both as longitudinal and shear waves, two theoretical models, namely, Maxwell and Voight models (Philipoff 1965) are used to analyse the mechanical relaxations. In Maxwell's model, the total deformation is taken as the sum of the viscous and elastic components while the shear stresses for the two processes are considered to be equal. In the Voight model, by contrast, the total stress is taken to be the sum of the viscous and elastic shear stresses but the resulting

deformations are considered to be equal. Equations (16) to (20) are based on Maxwell's model.

The discussion so far has been limited to a system with a single relaxation time. In real situations, as pointed out earlier, a distribution of such times exists and these relaxation times are described in terms of a reduced parameter, τ_s/τ_s'. Two such distributions often used correspond to the symmetric Gaussian and the asymmetric Davidson–Cole distributions. In the presence of these distributions, K', K'', η_v, G', G'' and η_s are defined by the integrals given in table 1.

In this article our intention is to focus on particle motions in the glassy state itself. As such, an analysis of the frequency dispersion of the shear modulus in the supercooled liquid is only of marginal interest to this article. Mechanical relaxation in the low-frequency region studied in internal friction measurements is more informative with respect to particle motions in glass.

We may note in passing that while the analyses of dielectric data are often performed using complex susceptibility, analyses of mechanical relaxations are done using complex modulus. More recently, however, the modulus representation is in vogue even in dielectric relaxation studies. This transformation is easily achieved by defining a dielectric modulus $M^* = M' + iM'' = 1/\varepsilon^*$. The resulting expressions are similar to those for mechanical relaxation (Wong and Angell 1976; Macedo *et al* 1972). In situations where the d.c. conductivity is large and is comparable to the a.c. conductivity, it is often advisable to treat the corrected conductivity ($\sigma_{\text{a.c.}} = \sigma_{\text{total}} - \sigma_{\text{d.c.}}$) itself as a complex quantity so that (Grant 1958; Daniel 1967)

$$\sigma^* = \sigma' + i\sigma'' = i\omega(\varepsilon' - i\varepsilon''). \tag{23}$$

Mechanical loss at low (10^{-2} Hz to 50 kHz) frequencies is often called internal friction which is identical to the loss angle or tan δ (Zdaniewski *et al* 1979). In this long-wavelength region where power dissipation is primarily through viscous flow, mechanical relaxation is advantageously described (Zdaniewski *et al* 1979) using the

Table 1. Mechanical properties for distributions of relaxation times.

$$K' = K_0 + K_r \int_0^\infty k(\tau/\tau_v')\omega^2\tau^2 \,\mathrm{d}(\tau/\tau_v')/(1+\omega^2\tau^2) \qquad G' = G_\infty \int_0^\infty \omega^2\tau k(\tau/\tau_s')\,\mathrm{d}(\tau/\tau_s')/(1+\omega^2\tau^2)$$

$$K'' = K_r \int_0^\infty k(\tau/\tau_v')\omega\tau \,\mathrm{d}(\tau/\tau_v')/(1+\omega^2\tau^2) \qquad G'' = G_\infty \int_0^\infty \omega\tau k(\tau/\tau_s')\,\mathrm{d}(\tau/\tau_s')/(1+\omega^2\tau^2)$$

$$\eta_v = K_r \int_0^\infty k(\tau/\tau_v')\tau \,\mathrm{d}(\tau/\tau_v')/(1+\omega^2\tau^2) \qquad \eta_s = G_\infty \int_0^\infty \tau k(\tau/\tau_s')\,\mathrm{d}(\tau/\tau_s')$$

Distribution functions used

(i) *Gaussian:*

$$k(\tau/\tau_{s(v)}') = b/\pi^{1/2}\cdot\tau_{s(v)}'/\tau\cdot\exp\left[-b\ln(\tau/\tau_{s(v)}')\right]^2 \qquad 0<\tau<\infty$$

(ii) *Davidson-Cole:*

$$k(\tau/\tau_{s(v)}') = \tau_{s(v)}'/\tau\,\sin(\beta\tau_{s(v)}'/\tau)\left[\tau/\tau_{s(v)}'/(1-\tau_{s(v)}'/\tau)\right]^\beta \qquad 0\leqslant\tau/\tau_{s(v)}'<1$$

compliances S_u and S_r where the subscripts u and r denote the unrelaxed and relaxed states. S_u can be written $S_u = 1/C_u$ and $S_r = 1/C_r$ in terms of the stiffness constants C_r and C_u. The complex compliance is $S^* = S' - iS''$, so that

$$\tan\delta = (S_r - S_u)/(S_r + S_u\omega^2\tau^2) \tag{24}$$

which may be compared with (5) in the dielectric case. For many solids, the relaxation strength, $\Delta = (S_r - S_u)/S_u$, is far less than 1 so that

$$\tan\delta = \Delta\omega\tau/(1+\omega^2\tau^2) \tag{25}$$

and $\tan\delta$ is therefore a symmetrical function of $\log\omega\tau$ centred about $\omega\tau = 1$. $\tan\delta$ is a measure of the absorption of vibrational energy in a solid (Fitzgerald 1951) and is also referred to as Q^{-1}, where Q is the quality factor. Experimentally it is determined by measuring the logarithmic decrement of vibrational amplitude of a freely vibrating solid, ϕ, where $\phi = \ln(A_0/A_n)$, $\tan\delta$ is then given by

$$\tan\delta = Q^{-1} = 2{\cdot}303\phi/n\pi, \tag{26}$$

where n is the number of cycles.

One of the basic modes of particle motion is vibrational. In the formalism that we have employed so far for dielectric and mechanical responses the expressions were relevant for time-scales far larger than vibrational time-scales. These time-scales, however, are themselves accessible to far infrared (FIR) spectroscopy (Wong and Angell 1976). The nature of absorption of energy from the impressed field has to be treated in the frame-work of a forced harmonic oscillator (Dekker 1967). If ω_0 is the frequency of a harmonic oscillator that is subjected to an alternating field of frequency ω, it can be shown that the complex dielectric constant arising from the polarization induced by elastic displacements is (Dekker 1967)

$$\varepsilon^* = 1 + [4\pi Ne^2/m((\omega_0^2 - \omega^2) + i\gamma\omega)]. \tag{27}$$

In (27) N, e, m, and γ are the number of particles per unit volume, the charge and mass of the particle and the damping constant (in units of ω^{-1}) respectively. The real and imaginary components may now be seen to be (Dekker 1967)

$$\varepsilon' = 1 + \{4\pi Ne^2(\omega_0^2 - \omega^2)/[(\omega_0^2 - \omega^2)^2 + \gamma^2\omega^2]\} \tag{28}$$

$$\varepsilon'' = 4\pi Ne^2(\gamma\omega)/m[(\omega_0^2 - \omega^2)^2 + \gamma^2\omega^2]. \tag{29}$$

It may be noted that absorption takes place only in the presence of the damping constant, γ, and this type of absorption is called 'resonant absorption'. While the absorption, *i.e.* ε'' or $\tan\delta$, peaks around ω_0 as in the case of relaxation, ε' (or more appropriately, $\varepsilon' - 1$) exhibits an anomalous dispersion (Lovell *et al* 1976). In solids it is more accurate to use ω_0 which is corrected for the presence of the Lorentz field and this is achieved by writing ω_1 for ω_0 where $\omega_1 = \omega_0^2 - (4\pi ne^2)/3m$ (Dekker 1967).

Since refractive index and dielectric constant are related, we can consider resonance absorption in terms of a complex refractive index, n^*, such that (Dekker 1967)

$$n^* = n - ik. \tag{30}$$

Noting that $n^{*2} = \varepsilon^* = \varepsilon' - i\varepsilon''$, it follows that

$$\varepsilon' = n^2 - k^2 \tag{31a}$$

and

$$\varepsilon'' = 2nk. \tag{31b}$$

It is conventional to measure absorbance $\alpha(\omega)$ in the high-frequency regime and $\alpha(\omega)$ is related to $\varepsilon''(\omega)$ by the expression (Wong and Angell 1976)

$$\alpha(\omega) = \omega\varepsilon''(\omega)/cn(\omega) \tag{32a}$$

where c is the velocity of light. ε'' may be related to the conductivity of the material through the relation (Wong and Angell 1976)

$$\sigma(\omega) = \omega\varepsilon_0\varepsilon''(\omega) \tag{32b}$$

where ε_0 is the permittivity of free space. Using this expression it is possible to evaluate conductivities at very high frequencies using values of the absorbance.

2.3 *Vibrational spectroscopy*

Particle motion in glasses, especially around the glass transition, can be profitably investigated using vibrational spectroscopy (Yarwood and Arndt 1979; Lascombe 1974). The band widths in IR and Raman spectroscopies, in particular, are influenced profoundly by molecular interactions. In the Schrödinger picture, transitions are regarded as taking place between well-defined states but in the Heisenberg approach attention is focussed on the time-evolution of these transitions so that the intensity of the band can be related to the appropriate correlation functions (Gordon 1965; Yarwood and Arndt 1979). It may be noted that both auto- and cross-correlation functions affect the band-shape but the latter are important only when motion is highly cooperative in nature. The shape of the correlation function, in principle, contains complete information about particle motion. Detailed accounts of the origin of band shapes and their analysis has been given by a number of authors (Gordon 1965, 1968; Bratos and Maréchal 1971; Young and Jones 1971; Nafie and Peticolas 1972; Bartoli and Litovitz 1972; Bailey 1974; Lascombe 1974; Yarwood and Arndt 1979). The two auto-correlation functions of interest to us are $\langle \mathbf{Q}_i(0)\cdot\mathbf{Q}_i(t)\rangle$ and $\langle \mathbf{u}_i(0)\cdot\mathbf{u}_i(t)\rangle$ where the **Q**'s are the normal coordinates of the ith molecule and the **u**'s are the unit vectors along the transition moment corresponding to the **Q**'s. If the normalised IR band intensity is written $\hat{I}_{IR}(\omega)$, a Fourier transform of the band is related to the correlation function by (Yarwood and Arndt 1979)

$$\Phi_{IR}(t) = \phi_v(t)\phi_{IR}(t) = \langle \mathbf{Q}_i(0)\cdot\mathbf{Q}_i(t)\rangle$$

$$\langle P_1[\mathbf{u}_i(0)\cdot\mathbf{u}_i(t)]\rangle = \int \hat{I}_{IR}(\omega)\exp(i\omega t)\,d\omega, \tag{33}$$

where $P_1 = \cos\theta_i(t)$ is the first order Legendre polynomial and $\theta_i(t)$ is the angle between the transition dipoles of the ith molecule at times 0 and t. In the case of Raman spectra obtained using a vertically polarized light source we have to consider both the vertically polarized scattered intensity (I_{VV}) and the horizontally polarized scattered intensity (I_{VH}). I_{VV} and I_{VH} contain information with respect to different correlation times and are related to isotropic ($I_{iso}(\omega)$) and anisotropic ($I_{aniso}(\omega)$) scattering intensities through the following expressions (Bartoli and Litovitz 1972).

$$I_{iso}(\omega) = I_{VV}(\omega) - (4/3)I_{VH}(\omega) \tag{34a}$$

$$I_{aniso}(\omega) = I_{VH}(\omega.) \tag{34b}$$

Corresponding correlation functions are given by (Yarwood and Arndt 1979)

$$\Phi_{\text{iso}}(t) = \phi_v(t) = \langle \mathbf{Q}_i(0)\cdot\mathbf{Q}_i(t)\rangle = \int_{\text{band}} I_{\text{iso}}(\omega)\exp(i\omega\tau)\,\mathrm{d}\omega \tag{35}$$

$$\Phi_{\text{aniso}}(t) = \phi_v(t)\phi_{2R}(t) = \langle \mathbf{Q}_i(0)\cdot\mathbf{Q}_i(t)\rangle\langle P_2[\mathbf{u}_i(0)\cdot\mathbf{u}_i(t)]\rangle$$

$$= \int_{\text{band}} I_{\text{aniso}}(\omega)\exp(i\omega\tau)\,\mathrm{d}\omega, \tag{36}$$

where $P_2 = \frac{1}{2}[3\cos^2\theta_i(t) - 1]$ is the second order Legendre polynomial. The auto correlation function corresponding to $\langle \mathbf{Q}_i(0)\cdot\mathbf{Q}_i(t)\rangle$ is known as the vibrational relaxation function (van Konynenburg and Steele 1975; Rothschild 1976; Doge *et al* 1977). While $\langle \mathbf{u}_i(0)\cdot\mathbf{u}_i(t)\rangle$ represents the reorientational correlation function (Yarwood and Arndt 1979). From the above equations it is obvious that

$$\phi_V^{\text{iso}}(t) = \Phi_{\text{iso}}(t) \tag{37a}$$

$$\phi_{1R}(t) = \Phi_{\text{IR}}(t)/\Phi_{\text{iso}}(t) \tag{37b}$$

$$\phi_{2R}(t) = \Phi_{\text{aniso}}(t)/\Phi_{\text{iso}}(t). \tag{37c}$$

In arriving at the above equations, it is assumed that the effect of a finite slit-width has been taken into account. Ignoring slit width effect is strictly incorrect.

A plot of the correlation function against time can be used to obtain the correlation time, τ_c which is defined by $\phi(\tau_c) = \phi(0)/e$ (figure 5). The correlation times obtained

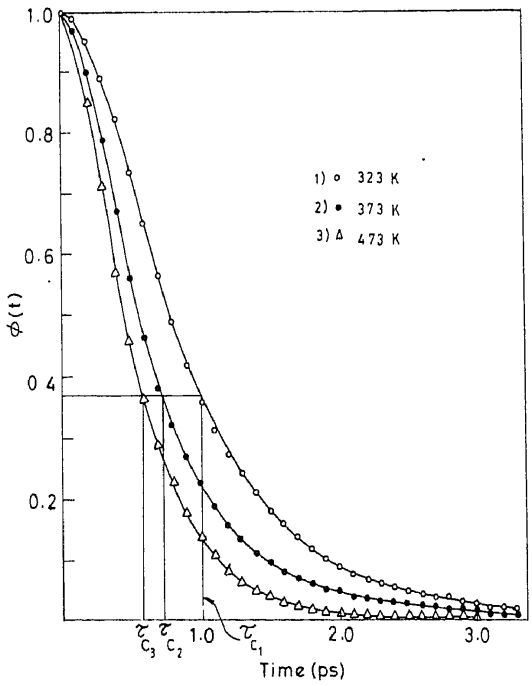

Figure 5. Variation of $\phi(t)$ with t for sulphate glasses at the temperatures indicated (see §3.6). Values of τ_c are also shown (after Sundar *et al* 1982).

thus from ϕ_{1R} (from IR) and ϕ_{2R} (from Raman) are the reorientational times. The correlation function $\langle \mathbf{u}_i(0)\cdot\mathbf{u}_i(t)\rangle$ is also often designated $\langle \mathbf{u}_i^{(2)}(0)\cdot\mathbf{u}_i^{(2)}(t)\rangle$ indicating that it is related to roto-diffusive motion.

Vibrational spectra can also be analysed in terms of band moments (Gordon 1965, 1968; Bailey 1974) since the correlation functions can be expanded in terms of a series of the moments. For a classical system consisting of relatively heavy molecules (Bailey 1974), the odd moments can be ignored and the correlation function may be written (Yarwood and Arndt 1979)

$$\phi(t) = 1 - [M_2 t^2/2!] + [M_4 t^4/4!] - [M_6 t^6/6!] + \ldots. \tag{38a}$$

where

$$M_n = \int_{\text{band}} (\omega-\omega_0)^n I(\omega-\omega_0)\,\mathrm{d}\omega \Big/ \int_{\text{band}} I(\omega-\omega_0)\,\mathrm{d}\omega. \tag{38b}$$

Many models of rotational and roto-diffusive motions have been described in the literature. Debye considered only small angle diffusive steps in his model (Debye 1929). Gordon developed a model of extended diffusion along similar lines (Gordon 1966). Gordon's M and J diffusion models correspond to cases where only orientations are randomized upon collision (M diffusion) and where the length of the angular momentum vector is also randomized (J diffusion). These models have been applied extensively and have been discussed by Kivelson and McClung (1968). The various τ values such as τ_J, $\tau_\theta^1 \equiv \tau_{1R}$ and $\tau_\theta^2 \equiv \tau_{2R}$ are related amongst themselves. In the perturbed limit of a free rotor, τ_θ (corresponding to the correlation time from the Debye model) is approximately equal to τ_J (Yarwood and Arndt 1979) and is itself approximated by the Stokes–Einstein relationship,

$$\tau_\theta \simeq 4\pi\eta a^3/3kT, \tag{39}$$

where η is the viscosity and a is the molecular radius. On the other hand, Kivelson and McClung (1968) have shown that τ_J for a spherical top molecule is given by

$$\tau_J = I_\alpha/8\pi K r_0^3 \eta, \tag{40}$$

where I_α is the moment of inertia (referred to the αth axis), K is a constant between 0 and 1 whose value is determined by the anisotropy of the molecular potential and γ_0 is the mean molecular radius. Equation (40) shows that $\tau_J \propto 1/\eta$.

2.4 *Spin resonance studies*

In glasses which contain either paramagnetic species or nuclei with non-zero spin, spin resonance experiments are of value in studying particle motions. A nuclear spin precesses about the axis of an applied magnetic field at its Larmor frequency, $\omega = \gamma H$, where γ is the nuclear gyromagnetic ratio and H is the applied field. The variation of the magnetization $\mathbf{M}$ of a material with time is given by (Pake and Estle 1973; Carrington and McLachlan 1967),

$$\mathrm{d}\mathbf{M}/\mathrm{d}t = \gamma\mathbf{M}\times\mathbf{H}. \tag{41}$$

The relaxation of magnetization along the three coordinate axes is given by the following equations known as the Bloch equations (Bloch 1946; Pake and Estle 1973)

$$\mathrm{d}M_x/\mathrm{d}t = \gamma(\mathbf{M}\times\mathbf{H})_x - M_x/T_2 \tag{42a}$$

$$\mathrm{d}M_y/\mathrm{d}t = \gamma(\mathbf{M}\times\mathbf{H})_y - M_y/T_2 \tag{42b}$$

$$dM_z/dt = \gamma(\mathbf{M} \times \mathbf{H})_z - (M_z - M_0)/T_1. \tag{42c}$$

T_1 and T_2 are known as the longitudinal or spin-lattice and transverse or spin-spin, relaxation times respectively and M_0 is the equilibrium magnetization. The Bloch equations are easily solved for the condition that an oscillating magnetic field is superimposed upon the static field. Expressions for the real, χ' and imaginary χ'', parts of the complex magnetic susceptibility $\chi^* = \chi' - i\chi''$ are given by the following equations (Carrington and McLachlan 1967; Schumacher 1970),

$$\chi'(\omega) = \tfrac{1}{2}\chi_0\omega_0 T_2(\omega - \omega_0)T_2/[1 + (\omega - \omega_0)^2 T_2^2 + \gamma^2 H_1^2 T_1 T_2] \tag{43a}$$

$$\chi''(\omega) = \tfrac{1}{2}\chi_0\omega_0 T_2/[1 + (\omega - \omega_0)^2 T_2^2 + \gamma^2 H_1^2 T_1 T_2] \tag{43b}$$

ω and ω_0 are defined by $\omega = \gamma H$ and $\omega_0 = \gamma H_0$ where H_0 is the value of the field at the absorption maximum (χ''_{max}). T_2 is related to the line-width and is given by (Poole and Farach 1971)

$$T_2 = 2/\gamma\Delta H^0_{1/2} = 2/\sqrt{3}\gamma\Delta H^0_{PP}, \tag{44}$$

where ΔH^0_{PP} is the peak-to-peak line-width in the derivative spectrum (assuming a Lorentzian profile of absorption). Determination of T_1, however, is more complex and needs saturation experiments. It may then be determined using ΔH *vs* P plots where P is the rf power. Knowing the slope, T_1 may be determined using the formula, $T_1 = \text{slope}/\gamma^2 T_2$ (Poole and Farach 1971). The origins of the line-broadening in magnetic resonance experiments generally fall into two categories *viz*, homogeneous and heterogeneous band-broadening. Homogeneous broadening occurs when the spin-levels between which the transition takes place are not clearly defined and are intrinsically broadened. This may occur either because of spin-spin dipolar interactions or spin-lattice interactions. 'Inhomogeneous broadening', however, describes an envelope of individual resonance peaks which are (shifted from their true position particularly by magnetic field inhomogeneities (Poole and Farach 1971). The dipolar interactions may be treated using the dipolar Hamiltonian, H_{DD} which (for the case of nuclear spin interactions) is given by (Carrington and McLachlan 1967),

$$H_{DD} = g_N^2\beta_N^2\left[\frac{\mathbf{I}_1 \cdot \mathbf{I}_2}{\gamma^3} - 3\frac{(\mathbf{I}_1 \cdot \gamma)}{\gamma^5}(\mathbf{I}_2 \cdot \gamma)\right], \tag{45}$$

which describes the interaction between two identical magnetic moments $g_N\beta_N I$ separated by a distance r. This line broadening mechanism dominates in many solids but is largely averaged out in fluids. Using a Boltzmann distribution for the population of the spin states it can be shown that (Carrington and McLachlan 1967),

$$(1/T_1) = W_1 + 2W_2, \tag{46}$$

where W_1 and W_2 are transition probabilities involving matrix elements of H_{DD}. Spins in the neighbourhood of the excited spin that are involved in random motion (both rotational and translational) cause random fluctuations at the site of the excited spin. An auto-correlation relaxation time, τ_c, of the random fluctuations can be defined that determines the value of T_1 and T_2 (Carrington and McLachlan 1967).

Of greater importance in glass is motional narrowing that occurs in NMR studies. We have already noted that T_2 is inversely proportional to $\Delta H^0_{1/2}$ or, equivalently (Wong and Angell 1976),

$$T_2^{-1} = \Delta\omega_0^2\tau, \tag{47}$$

where $\Delta\omega_0$ is the line-width corresponding to the rigid lattice and τ is the relaxation time. Atomic motions cause a decrease of the dipole-dipole interactions between the nuclei, thereby bringing down the value of τ_c and narrowing the resonance band-width. This type of narrowing has been treated by Bloembergen *et al* (1948) whose theory has been modified (Gutowsky and McGarvey 1952; Gutowsky and Pake 1950) to relate ν_j the jump frequency to $\Delta\omega$

$$\nu_j = (2\pi\tau)^{-1} = \alpha\Delta\omega/\tan\left(\frac{\pi}{2}\left(\frac{\Delta\omega}{\Delta\omega_0}\right)^2\right), \tag{48}$$

where α is a constant of the order of unity and $\Delta\omega_0$ is the line width when there is no motional narrowing. Since ν_j itself can be treated as a thermally activated quantity (Lidiard 1957; Poole and Farach 1971),

$$\nu_j = \nu_0 \exp(-E_a/kT). \tag{49}$$

The relation between τ_c and T which leads to band width narrowing with increasing temperature is at once apparent. A phenomenological model for motional narrowing has been developed by Hendrickson and Bray (1973) based on a two-state model. This yields the expression

$$\ln\left(\frac{1}{\Delta\omega} - \frac{1}{\Delta\omega_0}\right) = (-E_a/kT) - \ln(1/B - 1/\omega_0), \tag{50}$$

where B is the line-width associated with the excited state and may be related to the nature of the motion involved.

In ESR spectroscopy line-broadening mechanisms are again the spin-spin and spin-lattice interactions. The spin-lattice interaction is characterized by the relaxation time T_1 and may be looked upon as arising from two causes. In the first, the spin experiences magnetic field variations due to the dipolar fluctuations from lattice vibrations. In the second mechanism, proposed by Kronig (1939) and van Vleck (1939), variations in the local electrostatic fields are regarded as affecting the orbital motion of the electrons which in turn perturbs the energy levels in the paramagnetic species. This perturbation is sensed by the spin through spin-orbit coupling, thus providing a mechanism for spin relaxation. In general, $1/T_1$ is proportional to the square of the spin-orbit coupling constant, λ, and inversely proportional to the axial field splitting, δ, raised to a high power. The temperature dependence of spin-lattice coupling can also be quite different in different temperature ranges (Ayscough 1967).

Spin-spin relaxation is more directly explained. This may occur either through direct exchange in which case T_2 should be directly proportional to the exchange interaction energy J (or, $\omega_e = J/h$ the so-called exchange frequency) and inversely proportional to the square of the dipolar interaction E_{DD} (Ayscough 1967). Spin-spin coupling could also take place *via* the magnetic field of the spins themselves.

In solutions, however, relaxation of spin-half free-radicals and paramagnetic ions is governed by the anisotropy of the g-tensor, by spin-orbit interactions and also by dipolar coupling with the magnetic nuclei, (Carrington and McLachlan 1967; Ayscough 1967; Poole and Farach 1971; Pake and Estle 1973). It has been shown (Carrington and McLachlan 1967) that for the case of the anisotropic g-tensor T_1 and T_2 are governed by the relations

$$1/T_1 = (g' : g')\beta^2 H_0^2[12\tau_c/(1+\omega_0^2\tau_c^2)]/60\hbar^2 \tag{51a}$$

$$1/T_2 = (g' : g')\beta^2 H_0^2 [8\tau_c + 6\tau_c/(1 + \omega_0^2 \tau_c^2)]/60\hbar^2, \tag{51b}$$

where $(g' : g')$ denotes the inner product of the tensor with itself, $(g' : g') = \Sigma_{ik} g'_{ik} g'_{ki}$. The formulation of the relaxation mechanisms for paramagnetic ions and free-radicals with spins greater than half is, however, more complex and detailed discussions may be found elsewhere (Poole and Farach 1971).

2.5 *Mossbauer spectroscopy*

Mossbauer spectroscopy can also be employed very usefully to investigate particle motions in glasses. The particle motion is directly reflected in the Lamb Mossbauer factor or the recoil-free fraction, f, which is given by (Wertheim 1964)

$$f = \exp(-4\pi^2 \langle x^2 \rangle / \lambda^2), \tag{52}$$

where $\langle x^2 \rangle$ is the mean square amplitude of vibration in the direction of gamma-ray emission averaged over a time-interval equal to the life-time of the excited nuclear state and λ is the wavelength of the gamma ray photon. Since $\langle x^2 \rangle$ reflects the average displacement of particles from their mean position a temperature-variable study of the Mossbauer spectra of glasses should be quite informative particularly in the neighbourhood of the glass transition (Champeney 1979) where large-scale disturbances in particle positions may be expected. Other parameters such as isomer shift and quadrupole splitting also reflect the effect of motion but these effects are rather subtle and do not allow unequivocal interpretation by themselves.

3. Experimental studies

3.1 *Dielectric response*

Amongst the various methods used to study relaxation phenomena in glasses, dielectric relaxation is probably one of the most widely used (Owen 1963; Day 1974; Stevels 1977). We have already noted that dielectric relaxation is both temperature and frequency dependent so that one might expect to investigate relaxation behaviour by varying either temperature or frequency. The impressive amount of data gathered so far, does in fact demonstrate that both the variables have been exploited. The major sources of dielectric loss in glasses are (a) migration losses and (b) deformation losses (Stevels 1957; Owen 1963). It is to be expected that deformation losses are associated with the dipolar mechanism of charge storage and should, therefore, be common to molecular, covalent network and other types of glasses. Migration losses, on the other hand, should play a large role in modified network and in purely ionic glasses. In semiconducting glasses, electron hopping from site to site is the dominant source of dielectric loss (Lakatos and Abkowitz 1971; Thurzo 1975; Namikawa 1975; El-Bayoumi and MacCrone 1976; Mansingh *et al* 1972, 1975, 1976, 1978).

The subject of the dielectric behaviour of glasses has been reviewed excellently by Owen (1963) and more recently by Stevels (1977). In their study of pure fused quartz, Mahle and McCammon (1969) have found a dielectric loss peak at 1 kHz and at 25K which they attributed to the motion of network oxygens. Many technically important glasses which contain cations in a silicate or a borosilicate network exhibit dielectric loss peaks. The activation energy obtained from loss-maximum frequency vs reciprocal temperature plots is 0·7 eV (Stevels 1977). Taylor (1956, 1959) has also shown that the

activation barriers for dielectric relaxation and d.c. conductivity for several alkali silicate glasses are approximately equal indicating that the same motion is operative in both cases. A more recent review by Namikawa (1975) of a large number of silicate glasses, however, indicates that dielectric behaviour of glasses may actually be grouped in three categories. In the first category, a Maxwell-Wagner (Daniel 1967; Wagner 1914; Maxwell 1954) type of behaviour is postulated in which ions move over short distances with low activation energies. As a consequence, the barriers to a.c. and d.c. conductivities are vastly different. In the other two categories, ionic motion occurs over larger distances and the barriers to a.c. and d.c. conductivity are similar. The two categories, however, may be distinguished by the magnitude of a correlation factor, p, where p is defined as the ratio of $\sigma_{\text{d.c.}}$ to $\varepsilon_0(\varepsilon_s - \varepsilon_\infty)\,\omega_m$, where ω_m is the frequency at the loss maximum ($\sigma_{\text{d.c.}}$ and ω_m are referred to the same temperature). In figure 6a, b and c the behaviour of ε'' as a function of $\log f$ is shown for the three categories, and some examples are listed in table 2. Semiconducting glasses such as barium phosphotungstates also appear to exhibit migration losses very similar to those corresponding to long range diffusion of ions (Namikawa 1975).

The mechanism of ionic transport in glasses has been discussed by many workers using different models. Stevels and co-workers (Haven and Stevels 1956) have considered several mechanisms by which Na^+ can be transported in glasses such as free transport, vacancy transport, interstitial transport and interstitialcy transport corresponding both to short and long distances. Urnes (1967) has considered the possibility of a Grotthus-type mechanism being operative in glasses under the action of an electrical field. Both these models have, nonetheless, been criticized though they are capable of explaining at least qualitatively, the discrepancy between measured values of the diffusion coefficient, D, and those derived using the Nernst–Einstein equation

$$D/N = kT/ne^2. \tag{53}$$

A correlation factor, f, which is a measure of this discrepancy may be defined through the relation $D/N = fkT/ne^2$. Doremus has suggested that the deviation of f from unity is due to very fine scale phase separation. The presence of sub-microscopic heterogeneity has also been suggested by Terai and Hayami (1975). The low values of f that have been observed can occur when preferential paths are provided by such heterogeneities. In these models, the mechanism of d.c. conductivity would itself require the presence of both the fine scale phase separation and of different ranges of jump distances and would also require the operation of defect interstitialcy mechanisms. These facets of d.c. conductivity may be compared with several features of a.c. conductivity mentioned earlier. Thus materials where f is very different from unity should generally show Maxwell–Wagner losses.

Most alkali silicate glasses conform to a distribution of relaxation times of the Cole–Cole type with an α of about 0·4 (Namikawa 1975). The relaxation time spectra are reported to be fairly temperature independent (Taylor 1956, 1959). Semiconducting tungstate glasses also behave similarly. In molybdenum- and in vanadium-phosphate glasses, however, Mansingh and co-workers (1972, 1975, 1976) have shown that α has different values above and below the absorption peaks; for $\omega\tau \ll 1$, $\alpha = 0{\cdot}6$ while for $\omega\tau \gg 1$, $\alpha = 0{\cdot}4$. At very low temperatures, α tends to 0·9. A symmetric behaviour in log $\varepsilon''/\varepsilon''_{\max}$ *vs* log $(\omega/\omega_{\max})$ plots have been noticed by Hakim and Uhlmann (1971) who have discussed their results in terms of a distribution function suggested by Glarum.

Dielectric relaxation in borate and phosphate glasses have been studied by many

workers (van Gemert 1977; Quinten *et al* 1978; van Gemert and Stevels 1978). While pure B_2O_3 glass does appear to exhibit feeble dielectric relaxation (figure 7) alkali borate glasses exhibit dielectric peaks around 25K at a frequency of 1 kHz (van Gemert 1977). The height of the loss peak is approximately proportional to the alkali concentration upto 20 mol % beyond which it decreases. This has been correlated with the fraction of tetrahedrally coordinated boron atoms and the relaxation may then be viewed as a consequence of the motion of the alkali ions among the four identical planes of the tetrahedron. The loss is generally characterized as a deformation loss, or, more appropriately as loss due to local motions. Activation energies for such motion are low

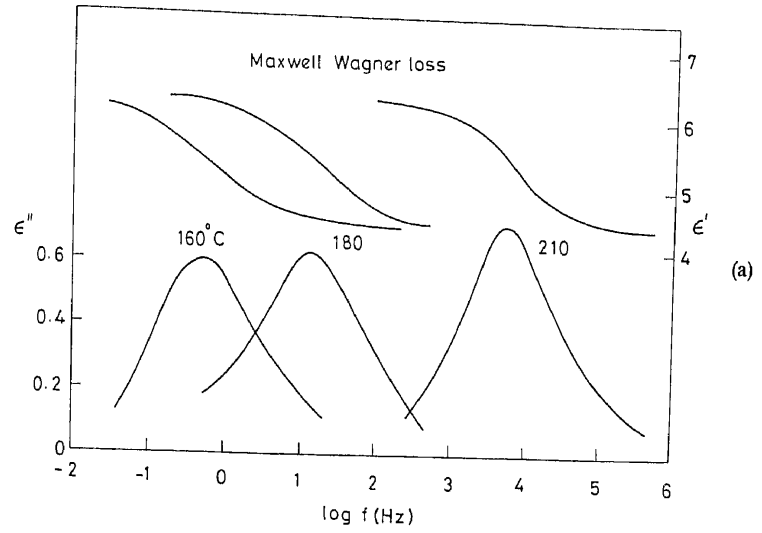

(a)

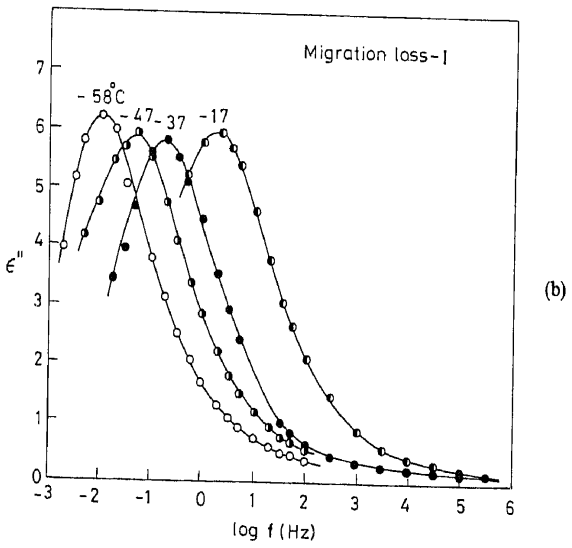

(b)

Figure 6. a, b.

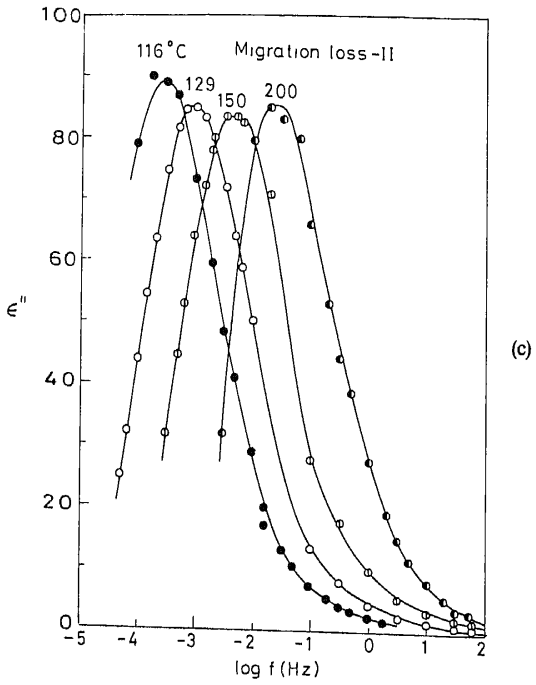

Figure 6. Typical dielectric relaxation based on (**a**) Maxwell-Wagner loss for an alkali borosilicate glass (**b**) migration loss (NLD) I for an alkali silicate glass (**c**) migration loss (NLD) II for an alkali silicate glass (after Namikawa 1975).

(*ca* 0·1 eV) (Stevels 1980). Similar losses due to local motion have been observed in silicates as well, where the activation barrier is *ca* 0·05–0·1 eV.

Dielectric relaxation studies of systems containing discrete anions are sparse. In their search for the so-called β-relaxations, Goldstein and co-workers (Johari and Goldstein 1970) found a loss peak at $\approx 0{\cdot}16\,T_g$ in a $Ca(NO_3)_2$-KNO_3 glass which, however, they did not regard as a β loss peak. At such low temperatures the β-relaxations are expected to be very diffuse. In this system as well as in the $Ca(NO_3)_2 \cdot 4H_2O$ system (Johari and Goldstein 1970) one may expect that the actual β peak is swamped by the large d.c. conductivity (Hayler and Goldstein 1977). In sulphate glasses the dielectric loss peak was observed just below T_g at a frequency of 1 kHz (Rao 1980). β-relaxation peaks are generally believed to be universal features of the glassy state (Wong and Angell 1976; Goldstein 1969; Johari and Goldstein 1970, 1971; Hayler and Goldstein 1977) and are associated with ionic motion between wells separated by low barriers (0·1–0·4 eV). In fact, a.c. conductivity measurements in sulphate glasses corroborate the presence of short range motion characterized by such barriers which are clearly much smaller than the activation barrier to d.c. conductivity (Sundar and Rao 1982b) ($\approx$ 1·0 eV).

Dielectric properties of many molecular organic glasses have also been investigated by Goldstein and co-workers. Glasses which have been studied are listed in table 3. A large number of these glasses exhibit β-relaxation around $0{\cdot}8\,T_g$ with a characteristically low activation energy of 0·1–0·4 eV (figure 8). β-relaxation may be explained convincingly in the frame-work of the cluster model. In this model glass is regarded as

Table 2. Electrical properties of some ionically conducting glasses.

Molar composition	$\log \sigma_0$[a] (Ω^{-1} cm^{-1})	$\Delta H_{d.c.}$ (kcal mol^{-1})	$\log f_{mo}$[b] (Hz)	ΔH_{dr} (kcal mol^{-1})	$\Delta\varepsilon$[c]	α[d]	p[e]
Localized diffusion (LD)							
1·2 Li_2O–28·2 B_2O_3–69·3 SiO_2	1·3	34·3	12·7	25·6	1·8	0·3	1
7·5 Li_2O–92·5 SiO_2	5·47	25·0	9·5	18·8	58	—	1
Non-localized diffusion I (NLD I)							
15 K_2O–85 SiO_2	1·24	18·3	11·8	17·8	22	—	1·2
30 Na_2O–70 SiO_2	1·92	14·5	12·5	14·0	17	—	1·4
30 Rb_2O–70 SiO_2	1·80	15·0	12·5	14·7	16	—	1·0
30 Cs_2O–70 SiO_2	1·18	16·0	11·5	15·7	17	—	3·2
Non-localized diffusion II (NLD II)							
15 Li_2O–15 K_2O–70 SiO_2	2·78	25·6	12·4	26·2	96	0·4	9
8 Na_2O–12 K_2O–10 CaO–70 SiO_2	2·56	26·4	11·2	26·1	317	0·4	10

[a] σ_0 denotes the pre-exponential factor in the expression $\sigma = \sigma_0 \exp(-\Delta H_{d.c.}/kT)$, where $\Delta H_{d.c.}$ is the activation barrier; [b] f_{mo} is the pre-exponential factor in $f_m = f_{mo} \exp(-\Delta H_{dr}/kT)$ where ΔH_{dr} is an activation barrier to dielectric relaxation and f_m is the frequency at the loss maximum; [c] $\Delta\varepsilon$ is the dielectric relaxation strength; [d] α is the Cole-Cole parameter; [e] p is a correlation factor.

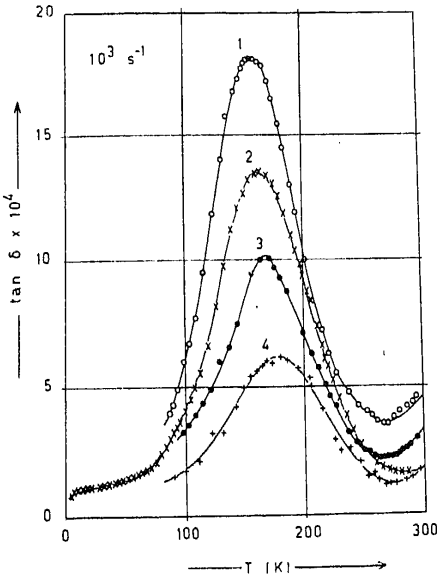

Figure 7. Tan δ versus temperature for B_2O_3 glass prepared from H_3BO_3 using different melting procedures: after heating at (1) 1000°C for 10 min (2) 1000°C for 30 min (3) 1000°C for 5 hr (4) 1200°C for 6 hr (after Quinten *et al* 1978).

Table 3. β-relaxations in some organic glasses.

Systems studied	T_g(K)	β-relaxation temperature, T_β, frequency	T_β/T_g
Rigid molecules:			
50 mol % *o*-fluorotoluene in *m*-fluorotoluene	121	Shoulder, 85K, 1 kHz	0.70
12 mol % chlorobenzene in *cis*-decalin	133	124K, 1 kHz	0·93
48·3 mol % 1-chloronaphthalene in tetrahydrofuran	111	112K, 500 Hz	1·0
38·1 mol % 1-chloronaphthalene in pyridine	147	103K, 1 kHz	0·7
Alcohols:			
2-Pentanol	133	104K, 10 kHz	0·78
3-Methyl-2-butanol	170	Shoulder, 150K, 10 kHz	0·88
Non-rigid molecules:			
Dimethyl phthalate	194	Shoulder, 175K, 1 kHz	0·90
Diethyl phthalate	184	157, 1 kHz	0·85
Isopropyl benzene	127	Shoulder, 115K, 1 kHz	0·91

consisting of clusters (regions characterized by a high degree of positional correlation) connected by tissue material of lower density within which particle motion is possible even below T_g (Goldstein 1975; Hayler and Goldstein 1979). Particle motion in such regions would then give rise to β loss peaks. It is worth noting that the cluster model has other significant implications in the phenomenology of the glassy state. Further, anionic motions in glasses should also contribute to dielectric losses at least at very low

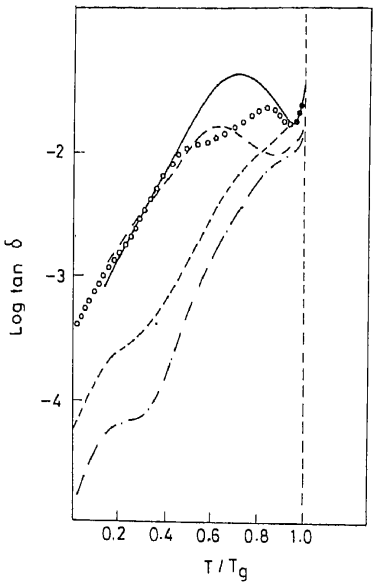

Figure 8. Variation of tan δ with T/T_g for a number of molecular glass systems: chlorobenzene in *cis*-decalin (– · – · –) (1 kHz); mixture of *o*- and *m*-fluorotoluene (– – – –) (1 kHz); 1-chloronaphthalene in tetrahydrofuran (O) (0.5 kHz); bromobenzene in tetrahydrofuran (— — —) (1 kHz); 1-chloronaphthalene in pyridine (———) (1 kHz). β-relaxations are clearly seen; low temperature anomalies are also evident in some cases (after Hayler and Goldstein 1977).

temperatures particularly when these ions are asymmetrically shaped. Investigations of anion motions and consequent dielectric loss behaviour in glasses, however, do not appear to have been reported.

3.2 *The mixed alkali effect*

'Mixed alkali effect' is the term used to describe non-linearities in the various properties of glasses with respect to composition containing more than a single-type of alkali ion (Isard 1969). Such deviations from linearity are particularly noticeable in properties connected directly with alkali ion motion (Isard 1969; Day 1974; Rao 1982). In dielectric loss measurements, for instance, the mixed alkali effect produces a pronounced dip in tan δ (Stevels 1951; Kostanyan 1960; van Ass and Stevels 1974a, b; van Gemert *et al* 1974; Sundar and Rao 1982a) and a characteristic loss peak in internal friction measurements (Zdaniewski *et al* 1979). In d.c. conductivity the mixed alkali effect gives rise to a clear minimum (Bartholomew 1973; Rao and Sundar 1980; Sundar and Rao 1982b) and to substantial alterations in alkali ion diffusivities (Terai 1971; Ohta 1975; Fleming and Day 1972) in a host of glasses; in other properties (*e.g.* molar volume), though, the mixed alkali effect is rather slight (Ivanov 1964; Caporali 1964). Figure 9 shows the mixed alkali effect as manifested in the various properties related to ionic motion in a range of glasses. The effect has been seen in both network (Day 1974) and discrete anion glasses (Rao 1982; Rao and Sundar 1980; Sundar and Rao 1982a). It can also be observed as a 'mixed anion effect' so that currently, it is often referred to as the 'mixed ion effect'.

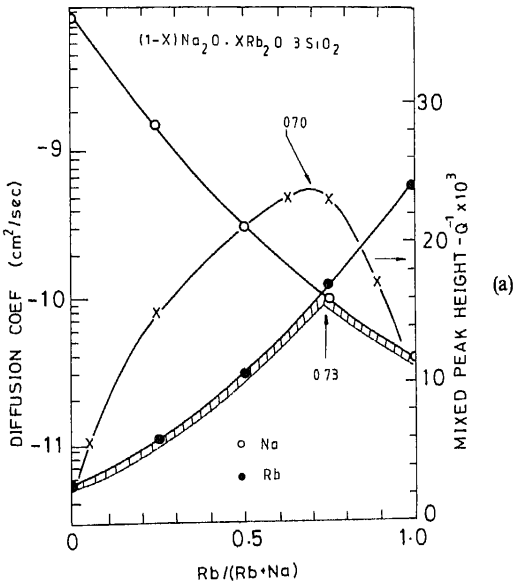
(1-X)Na2O · XRb2O 3SiO2
070
073
Na
Rb
DIFFUSION COEF (cm²/sec)
MIXED PEAK HEIGHT Q⁻¹ x10³
Rb/(Rb+Na)
(a)

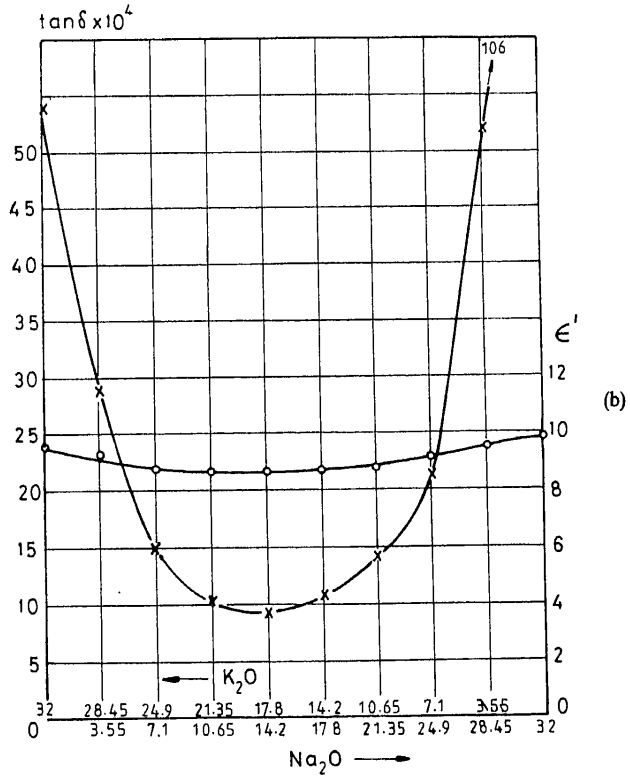
tanδ x10⁴
106
ε'
K2O
Na2O
(b)

Figure 9. a, b.

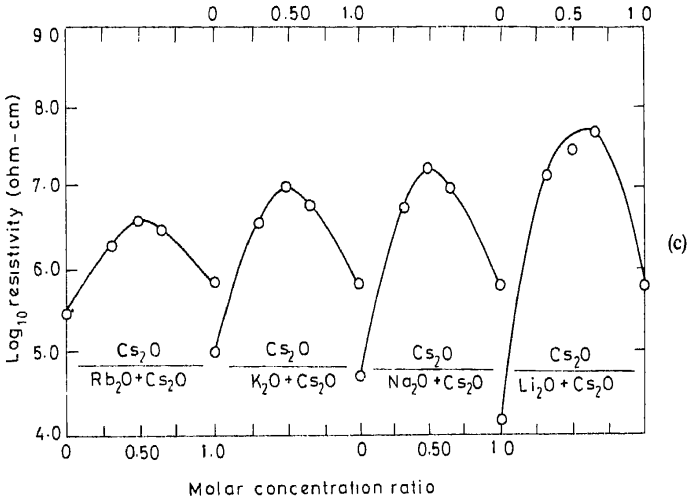

Figure 9. (**a**) Alkali diffusion coefficients and the mixed alkali internal friction peak as a function of composition in a mixed-alkali silicate glass. Cross hatch denotes the slower ion; (**b**) variation of $\tan\delta$ and ε' with composition in a mixed-alkali lead oxide–calcium fluoride–silica glass; (**c**) variation of resistivity with composition for various mixed-alkali silicate glasses (after Day 1976).

Many theoretical approaches have been made to explain the mixed alkali effect. These can be grouped under three heads *viz.* (a) structural (Stevels 1957; Charles 1965), (b) electrodynamic (Hendrickson and Bray 1972a, b) and (c) thermodynamic theories (van Gemert and Stevels 1978). Structural theories stress the importance of void sizes necessary for the transport of ions and consider the possibility of a blocking effect which reduces the effective mobility of the ions. In the electrodynamic theories the dissimilar masses of the ions (which give rise to dissimilar vibrational frequencies) develop an interaction energy due to the electrical fields of the vibrating ions. This energy affects the activation barrier and hence the motion of the ions. The thermodynamic theories consider that the simultaneous presence of ions of different sizes affects the total interaction energy and hence the migration barrier. Phase separation (Charles 1965), increase of pairing energies (Sakurai and Ooka 1968), anharmonicity of thermal vibrations (Weyl and Marboe 1962) and micro-strain fields (Rao and Sundar 1980) have all been considered as possible origins of the mixed alkali effect but, to date, no single model has proved to be either universal or quantitatively accurate in accounting for this motion dependent phenomenon.

The decrease in values of $\tan\delta$ in mixed alkali regions suggests two possibilities: (i) the ions stabilize in their own positions in response to the polarizing field or (ii) the consolidated motion of these ions in a sufficiently small region does not involve changes in polarization. As we shall see a little later, the latter possibility is consistent with the results of internal friction measurements.

3.3 *Mechanical relaxation*

Mechanical relaxation is measured using different techniques in different frequency ranges. Between 0·1 and 250 Hz it is measured by following the torsional oscillations of

a fibre, between 1 and 10 kHz by following the flexural vibrations of a bar and between 10 and 110 kHz by following longitudinal vibrations (Zdaniewski *et al* 1979). More recently, commercial instruments are used which can cover 4–5 decades of the entire internal friction measurement range (Atake and Angell 1980).

Single component network glasses such as SiO_2, B_2O_3 (Kurkjian and Krause 1968) and others exhibit very low energy losses. The losses are generally attributed to the network oxygen response and sometimes to the very small concentrations of impurities such as water. Ballaro *et al* (1975) for example, have observed a low temperature internal friction peak in silica glass with an activation energy of 0·05 eV in the megahertz region (figure 10). Binary alkali silicates have been the most extensively investigated and these, in general, exhibit two internal friction peaks (at $\sim$ 1 Hz); one between 233 and 248 K (Forry 1957; Ryder and Rindone 1960, 1961; Zdaniewski *et al* 1979) and the other between 373 and 573 K (Ryder and Rindone 1960, 1961; Shelby and Day 1969, 1970). The low temperature loss peak is believed to be due to alkali ion motion (generally referred to as the single alkali peak) since it has an activation energy (0·7–1·0 eV) very similar to that observed for d.c. conductivity in a number of glasses (Higgins *et al* 1972). The position of the second peak is dependent upon the nature of the modifying cation, silica content, traces of dissolved water etc., so that it is of uncertain origin. It has also been attributed to non-bridging oxygen ions (Rotger 1958), possibly because its magnitude has generally been found to be proportional to the alkali content (Forry 1957; Mohyuddin and Douglas 1960; Douglas 1963).

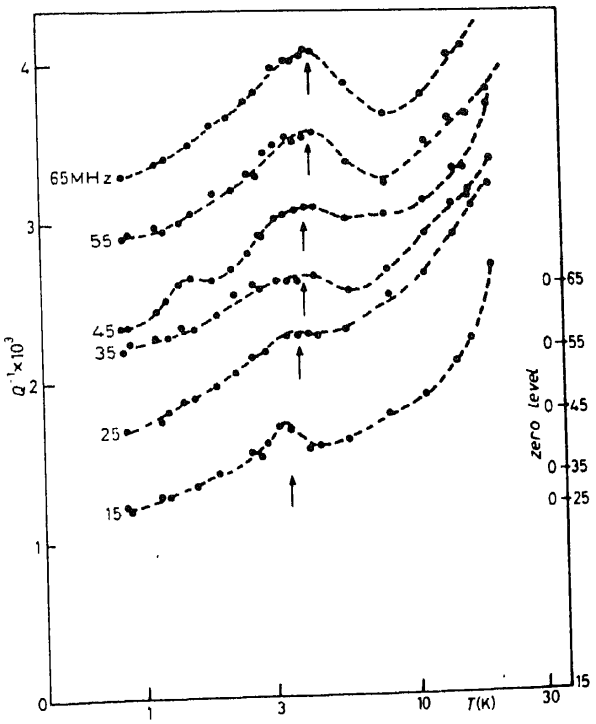

Figure 10. Internal friction coefficient as a function of temperature for SiO_2 glass at the frequencies shown. The ordinate scale for each frequency has been shifted upwards (scale on the RHS) (after Ballaro *et al* 1976).

The mixed alkali effect is very sensitively detected in internal friction experiments through the so-called 'mixed alkali peak' which appears (at $\approx$ 1 Hz) at a temperature slightly greater than that of the single alkali peak (Rotger 1941; Jagdt 1960). With increasing concentration of the second alkali the mixed alkali peak shifts to lower temperatures and its magnitude is also increased. Concurrently, the single alkali peak shifts to higher temperatures so much so that when the proportions of the two alkalis are comparable only a single, giant loss peak is observed (Zdaniewski *et al* 1979). We have pointed out earlier that the origin of mixed alkali relaxation is not very clear. Since the dielectric loss attains a minimum whereas a giant loss peak appears in internal friction it appears that the elastic dipole (formed from dissimilar alkali ions) is somehow rearranged in the a.c. stress field without causing alterations in electrical polarization. One is tempted to think that such a possibility ensues primarily from the rather high values of time constants in internal friction measurements as compared to the time scale of polarization renormalization.

Internal friction losses have also been noted at very high frequencies (megahertz region) in glassy selenium and GeS_2 (Carini *et al* 1978). An absorption minimum has been noted for these materials at 150 K and 450 K respectively which the authors have discussed in the light of a 'stochastic resonance absorption' model. Mechanical relaxations of a variety of metallic glasses have also been investigated. Tyagi and Lord (1979) have measured the internal friction of $Fe_{24}Ni_{40}P_{14}B_6$, $Fe_{29}Ni_{49}B_6Si_2P_{14}$ and $Fe_{80}B_{20}$ glasses at frequencies of 0·2 and 1 Hz. The increase in internal friction with temperature yields an activation energy of 40–80 kcals mol^{-1} which the authors attribute to unspecified atomic motions.

Ultrasonic studies of glasses, particularly silica (Golding *et al* 1973; Hunklinger *et al* 1972) and some chalcogenides (Ng and Sladek 1975; Farley and Saunders 1975) have revealed an anomalous saturation of the ultrasonic attenuation at very low temperatures. Many other physical properties, such as heat capacity (Fislia *et al* 1969), also behave anomalously in this temperature range. Theoretical approaches to the problem were first made by Anderson and Bommel (1955) and later by Anderson *et al* (1972). It seems that these anomalous features may be explained if we assume the existence of two-state potential wells separated by low energy barriers (asymmetric double well potential) (Phillips 1972). Particle motion between these wells can occur either by tunnelling through or by hopping over the barrier. The model is sufficiently general so that it can be used to account for various anomalies through an imaginative use of structural data. Indeed, the low temperature anomalies in fused quartz have been attributed by Anderson and Bommel (1955) to the displacement of SiO_4 tetrahedra which is consistent with the random network model proposed for these glasses. In borosilicate glasses too, studies by Arnold *et al* (1974) have indicated the presence of such anomalies. Currently, it is believed that such anomalies are a fundamental property of glasses and attempts have been made to correlate the glass transition temperature with the density of such energy-split states (Raychaudhari and Pohl 1981; Cohen and Grest 1981).

3.4 *The glass transition and associated relaxations*

We have pointed out earlier that pronounced dielectric loss occurs near the glass transition. Very similarly internal friction studies also show loss peaks which are known as α peaks that generally tend to appear at temperatures above the calorimetric glass

transition temperature. The glass transition itself marks the onset of flow properties and is associated with steep variations in heat capacity, thermal expansivity and compressibility of the material (Rao 1979). It is also the temperature above which the rate of acquisition of entropy by the system is higher. A consideration of the glass transition as it occurs upon supercooling of liquids is even more informative. The glass transition then corresponds to the kinetic 'freezing' or the falling out of equilibrium, of the metastable supercooled liquid. It is at once obvious that the 'freezing' is a time dependent phenomenon which logically leads to the postulation of a 'fictive temperature' (Hagy and Ritland 1957; Haddad and Goldstein 1978). This is a structure related temperature and can be regarded as that temperature where the structure of the glass is, in fact, its equilibrium structure. Consequently, the fictive temperature of a glass and the relaxations around T_g are related to each other. When a glass is brought rapidly to a temperature above the fictive temperature it relaxes to the equilibrium structure with a characteristic relaxation time spectrum. Many experiments have been designed to follow the relaxations at T_g including measurements of refractive index (Macedo and Napolitano 1967), density (Ritland 1954), thermal expansivities (Hagy and Ritland 1957; Williams and Angell 1973) and heat capacities (Boehm *et al* 1981). In general, the relaxation time may be related to the fictive temperature as (Narayanaswamy 1971),

$$\tau = A \exp\left[(x\Delta h/RT + (1-x)\Delta h/RT_f)\right], \tag{54}$$

where a, x and Δh are constants and T_f is the fictive temperature. It is clear that as T tends to T_f, τ has essentially an Arrhenius dependence which corresponds to small displacements from equilibrium. The relaxation in this region is generally described as non-linear response (Wong and Angell 1976) and we do not propose to discuss it further in this article. However, we give below a summary of our understanding of the kinds of motion that characterize T_g mostly for purposes of completeness.

Relaxation times become very large as a supercooled liquid approaches T_g. Since cooling leads to a considerable decrease in volume and entropy, configurational rearrangements that take place near T_g become increasingly difficult and more cooperative (Barlow *et al* 1966; Rao 1979). Over a substantial range of temperature, transport properties of the supercooled liquid are non-Arrhenius and may be represented by the well-known Doolittle (1951) or Vogel-Tammann-Fulcher (VTF) (Vogel 1921; Tammann and Hesse 1926; Fulcher 1925) equation,

$$\phi = \phi_0 \exp\left[\pm B/(T-T_0)\right] \tag{55}$$

where ϕ is the transport property being measured and B is usually an activation barrier and T_0 a constant with units of temperature. Most theories of the glass transition have addressed themselves to an explanation of such a temperature dependence and to an identification of T_0 with a truly thermodynamic glass transition temperature (Kauzmann 1948; Rao 1979). The experimental glass transition, however, occurs beyond T_0 and corresponds to the 'freezing-in' of excess quantities such as entropy or free volume. The non-linear relaxations alluded to above are associated with these frozen-in excess quantities (Wong and Angell 1976).

Considerable effort has also been expended in the literature on a discussion of the so-called 'order parameters' (Cooper 1977; Gupta and Moynihan 1976, 1978; Kovac 1981) which can be any of the excess quantities that determine the free energy of the liquid and hence the glass transition temperature. (It has been conventional to use the term 'order parameter' in phase transitions so that it denotes a perfectly ordered state when equal to

unity. The order parameter cooperatively vanishes at the transition temperature. In the context of the glass transition it is preferable to designate the excess quantities of the supercooled liquid as 'order*ing* parameters' after Cooper (1977)). It has been known for a long time (Davies and Jones 1953) that the Prigogine-Defay ratio, π, for the glass transition is either equal to or greater than unity depending upon whether a single ordering parameter or a multiplicity of ordering parameters govern the glass transition (π is defined as equal to $(\Delta\alpha)^2/TV\Delta C_p\Delta\beta$ where $\Delta\alpha$, ΔC_p and $\Delta\beta$ are changes in thermal expansivity, heat capacity and compressibility respectively at T_g). Further constraints upon ordering parameters that determine the value of π have been investigated by many workers (Kovac 1981; Gupta and Moynihan 1976).

A model of the glass transition that is particularly attractive in the context of the α relaxations has recently been discussed by Perez *et al* (1981). Their approach is largely based on Goldstein's model (Goldstein 1975; Hayler and Goldstein 1977) that considers glass as consisting of dense clusters embedded in connective tissue of lower density. Particle motion is then considered to occur within the tissue material and/or on cluster boundaries. From an elaborate consideration of relaxation time spectra and internal friction losses as a function of temperature Perez *et al* (1981) have attributed the β loss peaks to cooperative rearrangements in the tissue material and α relaxations to thermally activated particle motion on cluster surfaces.

3.5 *Magnetic resonance spectroscopy*

Studies which have used magnetic resonance spectroscopy to understand particle motion in the glassy state are relatively few in number. Even these investigations have concentrated, specifically, either on ionic motion *per se* or on the anomalous behaviour of T_1 (the spin-lattice relaxation time, discussed in §2.4) due to the two-level systems (TLS).

The work of Bray and co-workers on NMR studies of ionic motion in glass has been truly monumental. In silicate and borate glasses, for example, Hendrickson and Bray (1974) have used ^{7}Li NMR to explore the behaviour of the spin-lattice relaxation time. A semilog plot of inverse corrected linewidth *vs* $1/T$ (figure 11) obtained in $Li_2O \cdot 2SiO_2$ glass clearly shows the presence of motional narrowing which has been analysed in terms of equation (50). Three straight line segments (denoted by I, II and III) are evident in the plot with region II having the highest slope and, consequently, exhibiting the highest activation energy. Region I has been attributed by the authors to short range motion which has a smaller activation energy and higher values (10^{-1} to 10^{-4} kHz) of B, as in (50). In region II the activation energy is about 0·6–0·7 eV and the B value is much smaller ($\sim 10^{-12}$ kHz); the latter feature has prompted the authors to associate this region with predominantly long range motion of the alkali ion. It is interesting to note that motional narrowing in the glassy region indicates two distinct regimes for ionic motion. There is a close correspondence between these results and those of dielectric relaxation discussed earlier. Hendrickson and Bray (1974) have further pointed out that the short range motion of the alkali ion could possibly be associated with equivalent sites on the SiO_4 or BO_4 tetrahedra. In any event, such short range motion is evidently a feature of the vitreous state since region I does not appear on similar plots made for crystalline samples.

^{11}B NMR and spin lattice relaxation has been studied in the case of glassy B_2O_3 and B_2S_3 through the glass transition and well into the supercooled region (Rubinstein

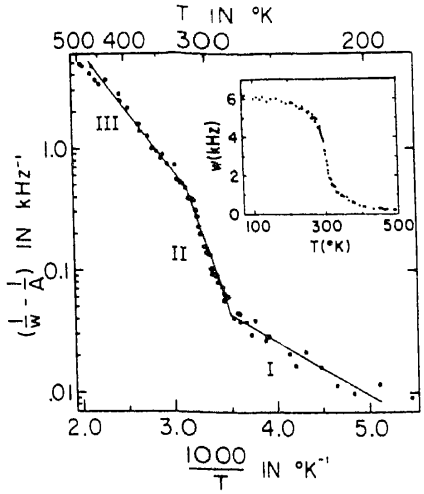

Figure 11. A plot of log inverse corrected ^{7}Li linewidth *vs* $10^3/T$ for Li_2O-$2SiO_2$ glass. Inset: the measured linewidth as a function of temperature, which clearly shows motional narrowing (after Hendrickson and Bray 1974).

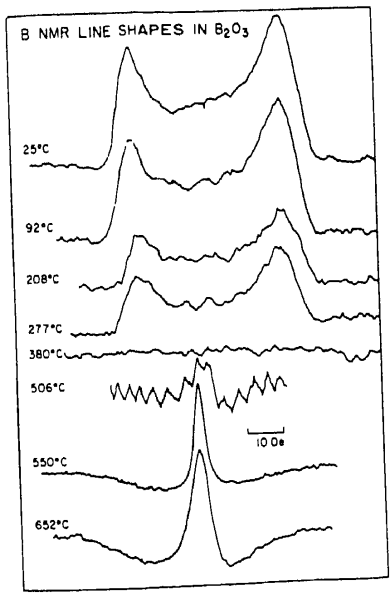

Figure 12. Changes in the ^{11}B NMR spectrum in amorphous B_2O_3 as a function of temperature (after Rubinstein 1976).

1976). Figure 12 shows the dramatic spectral changes that ensue, particularly at T_g for B_2O_3. While the central narrow line emerges only beyond T_g ($\sim$ 550 K) in the oxide, it evolves gradually at the expense of the 'powder pattern' in the sulphide even below T_g ($\sim$ 375 K). In fact, an extremely narrow line has been observed in glassy B_2S_3 just

25°K above the glass transition. The author suggests that the structures of the two glasses are very similar but that B_2S_3 behaves as a molecular fluid beyond T_g.

Rubinstein and Resing (1976) have also reported NMR studies which are related to TLS in glassy as well as in polycrystalline B_2O_3. An anomalous low minimum has been observed in T_1 which is mildly frequency dependent. From figure 13 which shows T_1 as a function of temperature for both the crystal and the glass, it becomes clear that relaxation is $\approx$ 30 times faster in the glass than in the crystal. The authors have analyzed their observations in terms of asymmetric double-well potentials which were earlier used to rationalise the existence of low temperature thermal anomalies. Figure 13 also shows a minimum in T_1 and this has been discussed in terms of temperature dependent broadening of the phonon spectrum which, in turn, causes a decrease in the effective density of states. Szeftel and Alloul (1978) have studied nuclear magnetic relaxation in Se, B_2O_3, borate and borosilicate glasses using ^{77}Se, ^{11}B, ^{23}Na and ^{29}Si NMR in very low temperature region. These workers have observed that T_1 is field independent and that it has a complicated temperature dependence of $1/[T^{(1+\gamma)}]$ where $0 \leqslant \gamma \leqslant 1$. They have also confirmed the presence of T_1 minimum in B_2O_3 at 300 K but most importantly they attribute the relaxation time behaviour to an electric field fluctuation at the nuclear site due to the tunnelling of nearest neighbour defects. These defects have tentatively been identified as bridging oxygens tunnelling between a pair of potential wells.

Muller-Warmuth and Otte (1980) have recently reported a study of nuclear magnetic spin relaxation in a number of organic compounds. In an investigation of solutions of

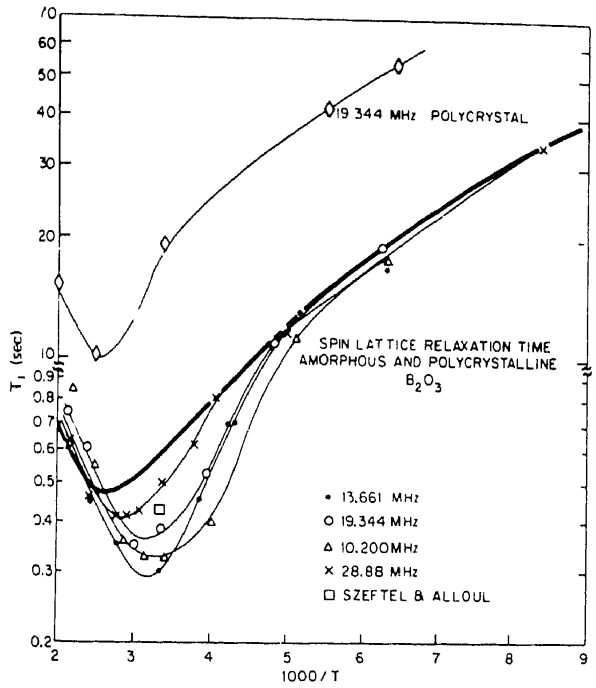

Figure 13. The spin-lattice relaxation time as a function of temperature in both glassy and crystalline B_2O_3 (after Rubinstein and Resing 1976).

benzene and substituted benzenes in glass-forming solvents such as *o*-terphenyl, *cis*-decalin and benzophenone, they found a minimum in T_1 around 100 K. Such an anomalous decrease in T_1 has been analysed in terms of distribution of correlation times and has been attributed to the characteristic low-lying excitations present in amorphous systems. The activation energy of such correlation times was found to be generally very low ($\approx$ 0·1 eV).

Motional narrowing can play an equally significant role in ESR spectroscopy as is evident from a recent study by Antsiferova *et al* (1973) of an organic free radical (PADS) in supercooled aqueous glycerol. They have compared simulated line-shapes obtained using various models with experimental results and have concluded that the jump diffusion model (§3.5) is more appropriate to a viscous medium than the Brownian motion model. It is quite curious that ESR studies have not so far been widely used to study particle motion in the vitreous state. Some work in this direction has recently been initiated in our laboratory (Parthasarathy *et al* 1981a) both in organic and in inorganic glasses primarily to gather information on particle motion in the neighbourhood of T_g. Such data, it was felt, would be vital to an understanding of the glass transition itself. It must, however, be emphasized that analysis of all the dynamical features associated with the non-linear relaxation region through ESR relaxation times is avowedly difficult. The variation of relaxation time *per se* with temperature should nonetheless reveal the evolution of liquid-like behaviour within the glass.

Experiments on organic glasses were made using an ESR spin-probe, TEMPONE (2,2,6,6-tetramethyl-piperidin-4-one-1-oxyl) which was dissolved in the liquid under study at a concentration of $\approx 10^{18}$ spins cm^{-3}. Transverse correlation times of this probe were then studied through the glass transition. The spectra of TEMPONE in glycerol and in methyl salicylate are shown in figure 14a, b. Correlation times, τ_c, were obtained using

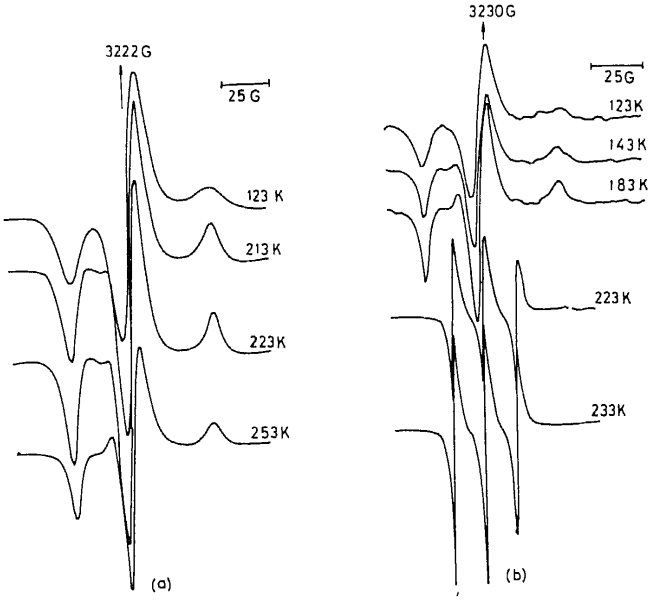

Figure 14. ESR spectra of TEMPONE in (**a**) glycerol and (**b**) methyl salicylate at selected temperatures (after Parthasarathy *et al* 1981).

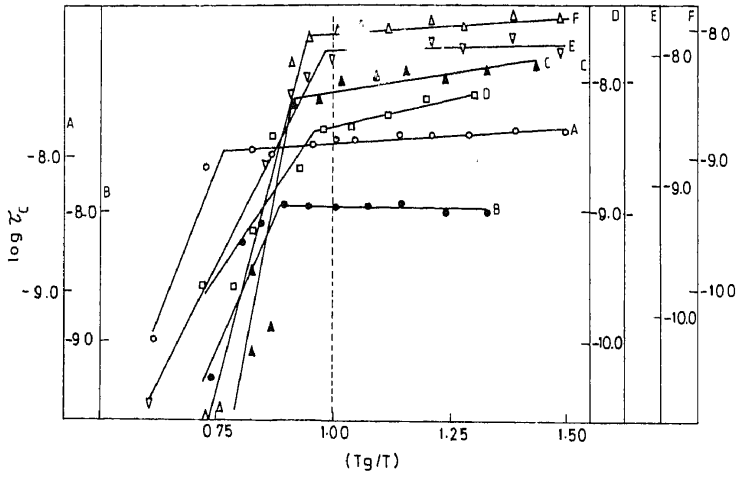

Figure 15. A plot of log τ_c against T_g/T for A: glycerol; B: *o*-toluidine; C: methyl salicylate; D: propylene carbonate; E: dimethyl phthalate; F: *p*-anisaldehyde. The broken line indicates T_g (after Parthasarathy *et al* 1981).

the procedure of McConnell (Stone *et al* 1965) and the variation of log τ_c with T_g/T is shown in figure 15 for all the liquids studied. It is clear that upto a temperature T_k, where $T_k \geqslant T_g$, τ_c is rather large and generally independent of temperature. In the supercooled region where $T > T_k$, τ_c decreases rapidly. The authors have rationalised their observations using the cluster model of glass, elements of which were discussed earlier in this section. In this model, the glass transition may be considered to correspond to a 'congelation' of clusters as the melt is cooled. The existence of a considerable amount of less dense, intercluster tissue material is, of course, assumed. The TEMPONE radicals being themselves heterogenities were considered to act as nuclei which eventually grow into clusters upon cooling. It is for this reason that their correlation times were seen to increase rapidly in the supercooled region and reach values characteristic of the glass well above T_g (at T_k). It is quite likely that the extent of hydrogen bonding is at least partially responsible for the deviation of T_k from T_g and, hence, for the different values of T_k observed in the various glasses. The activation energy obtained from the supercooled region ranged from 0·6 to 3 eV.

In inorganic glasses, transition metal ions may be effectively used as spin probes. The large relaxation times of Mn^{2+} and Fe^{3+} have been exploited in a study of the glass transition in 3 glasses: a discrete anion sulphate glass, a covalent network phosphate glass and a complex $PbO\text{-}PbCl_2$ glass of intermediate ionicity (Parthasarathy *et al* 1981b). Surprisingly, it was found that the line widths were constant through the glass transition, showing thereby no motional narrowing effects (figure 16). One wonders whether motional narrowing was offset by line broadening mechanisms operating in glasses with relatively high T_g's or whether such narrowing takes place in the supercooled liquid at temperatures which were not accessible to these workers. However, it was noticed that the resonance strength decreased rapidly through the glass transition. The decrease in resonance strength has, nonetheless, been discussed indirectly in terms of transverse relaxation times which were related to a function of inverse configurational entropy values of which were obtained theoretically from a two-state model (Angell and Rao 1972).

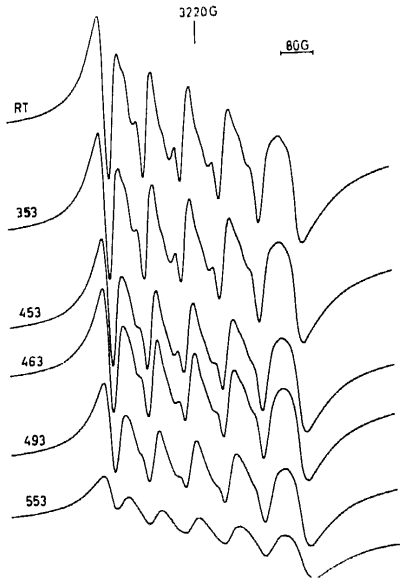

Figure 16. Variation of the ESR spectrum of Mn^{2+} in a sulphate glass ($T_g \simeq 460$ K) at selected temperatures (after Parthasarathy *et al* 1982).

3.6 *Vibrational spectroscopy*

The discussion in §2.3 indicated the possibility of using vibrational spectroscopy very effectively to understand particle motion in the glassy state. Little, however, appears to have been accomplished in this direction (Angell 1980). Rothschild (1974) has recently analysed the 1033 cm^{-1} ring deformation band in quinoline in the crystalline, liquid and glassy states. He has found that relaxation in this molecule is primarily vibrational. Relaxation times appear to be much higher in the crystalline rather than in the glassy state where the wide distribution of environments may promote effective relaxation.

Reports of other recent vibrational band shape studies in viscous liquids and glasses has been reviewed by Angell (1980). Raman studies of organic (toluene) and inorganic (KNO_3-$Ca(NO_3)_2$) glasses have been reported (Clarke and Miller 1972). While very little heterogeneous band broadening has been found above T_g in the case of toluene, band broadening appears to be substantial in the case of the nitrate glass.

The behaviour of IR band shapes has been investigated in a sulphate glass (Sundar *et al* 1982) in order to understand particle motions around T_g, using the 620 cm^{-1} sulphate deformation mode. Surprisingly, the band-width was found to increase upto T_g and thereafter, it remained constant. Correlation times, were obtained using the Fourier methods discussed in §2.3, and these are shown as a function of T/T_g for a number of compositions in figure 17. Second moments were also evaluated using (38b) and it was found that these reached saturation values just below T_g in all the compositions. The kind of saturation behaviour observed both in τ_c and second moments appears to indicate that liquid-like particle motion evolves in glasses at temperatures less than T_g. This would indeed be quite consistent with a cluster model of glasses and the glass transition discussed earlier since it is possible that melting of the inter cluster material prior to T_g would give rise to the observed behaviour.

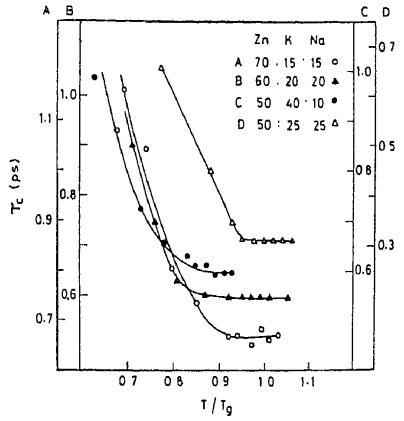

Figure 17. A plot of τ_c, obtained from IR band-shape analysis, as a function of T/T_g for sulphate glasses whose molar compositions are as shown (after Sundar *et al* 1982).

3.7 *Mossbauer studies*

A number of interesting Mossbauer studies, particularly through the glass transition, have been reported in the literature. One of the earlier studies is by Cooper and co-workers (Gosselin *et al* 1968) who studied the Mossbauer spectra of a sodium trisilicate glass containing 8·25 wt % of Fe_2O_3 through the T_g. They have reported that the line width of the Fe^{2+} resonance is unchanged while that of Fe^{3+} broadened. Recoil-free fraction, isomer shift (IS) and quadrupole splitting (QS) were observed to decrease with increase in temperature. More recent studies have confirmed that changes in these parameters, *viz*, recoil-free fraction, Lamb-Mossbauer factor, line-width, IS and QS through the glass transition are, in fact, quite generally found (Champeney 1979). Figure 18 shows the general behaviour of recoil-free fraction as a function of temperature for both glassy and crystalline states.

In their studies of Fe^{2+} ions in glycerol, Abras and Mullen (1972) have found evidence for the broadening occurring both due to jump and continuous diffusion of particles depending upon temperature. A more recent report on x-ray attenuation and Mossbauer line broadening in an aqueous phosphoric acid solution of Fe^{2+}, however, presents evidence against the jump model (Ruby *et al* 1975). Barnes and Langevin (1963) have investigated a frozen aqueous solution (FAS) of an ion salt and have noted that the recoil-free fraction decreases continuously with temperature and vanished at T_g (210 K). Brunot *et al* (1971a, b) also report similar findings in their FAS studies. The decrease in recoil-free fraction at the T_g has also been recorded by Simopoulos *et al* (1970). Yet another recent report of the Mossbauer study of ferrocene in *o*-terphenyl (Vasquez and Flinn 1980) notes that while $\langle x^2 \rangle$ decreases at T_g, line-broadening is not significant at temperatures just greater than T_g (figure 19). A significant point made by these workers is that values of the glass transition temperature obtained through studies of transport properties such as diffusion and viscosity should be distinguished from those obtained from static properties such as specific volume, enthalpy or power spectrum.

A qualitatively different approach to the problem has been adopted by Ruby and co-workers in their reports of Mossbauer studies on ferrocene in butyl phthalate (Flinn *et*

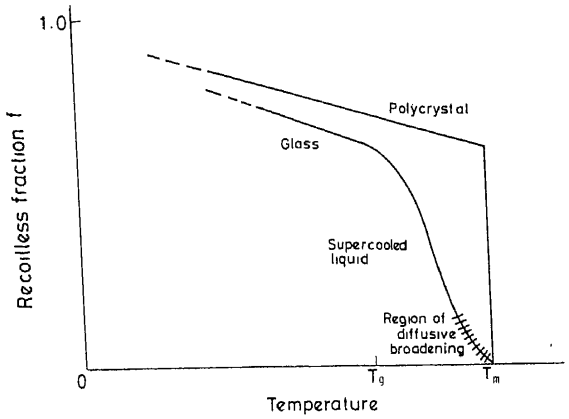

Figure 18. A schematic diagram of the variation of the recoil free fraction as a function of temperatures. It may be noted that diffusive broadening in glasses takes place well beyond T_g (after Champeney 1979).

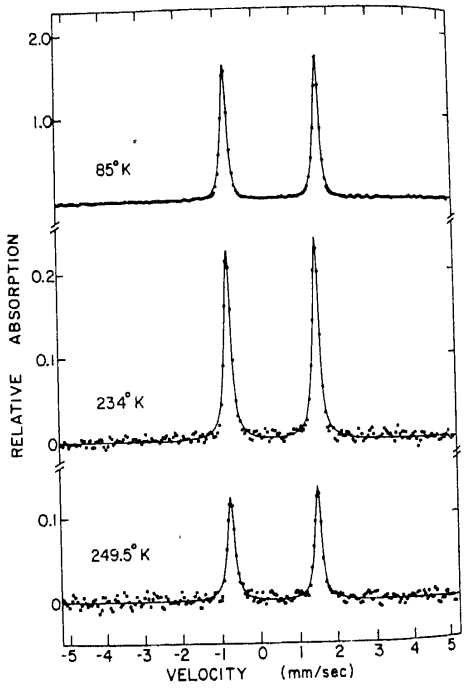

Figure 19. Mossbauer spectra of ferrocene in *o*-terphenyl for selected temperatures. While the recoil free fraction decreases rapidly beyond the T_g, it is significant that the line width shows no clear-cut increase (see figure 18) (after Vasquez and Flinn 1980).

al 1976; Ruby *et al* 1976) and phosphoric acid. They have observed an increase in $\langle x^2 \rangle$ beyond T_g but they note that rotational relaxation is unlikely to be observed in Mossbauer studies. Even more interesting, however, is their interpretation of the

decrease in elastic scattering intensity in terms of 'soft modes' as interpreted in the context of glasses. As Flinn *et al* (1976) remark, 'It is not that (such) transverse modes of the liquid gradually disappear with decreasing viscosity, but they are shifted to lower energies'. Considering the exciting possibilities that such an approach opens up and the fundamental importance of soft modes themselves, we feel that a brief digression on the soft mode postulate will not be out of place here.

The concept of soft modes as a basis for understanding phase transitions in solids has been developed over the last two decades and has provided a unifying structural approach to phase transformations (Rao and Rao 1978). The softening of vibrational modes or of elastic stiffness constants, it may be noted, has long been recognized as an origin of lattice instability (Born and Huang 1954). In the present context the applicability of the notion of phonons to disordered solids has been discussed by many authors and has been excellently summarized by Wong and Angell (1976). It is also known that the glass transition corresponds to the onset of the loss of solid-like rigidity as the vitreous solid undergoes transition. Against this background, therefore, it is attractive to consider that the decrease in force constants of some phonon modes, at the glass transition, gives rise to large amplitude motion of particles which is, essentially, the feature of a soft mode. Unlike solid-solid transformations, no new vibrational modes may be expected to appear at the T_g, which would strengthen and stabilize a new phase. It is also worthwhile to note that there may not be complete softening of all the modes at T_g since the properties of the vitreous state are characterized by distribution functions. In this context, it is likely that long- and short-range phonons in a glass are also governed by a distribution of force constants which may not concertedly soften. Thus, the soft mode that may drive a glass transition is quite likely to be different in its details from the soft mode that drives crystalline transitions, a point made by Flinn *et al* (1976). The advantage in the soft-mode approach is that it provides a novel method of describing the glass transition as it occurs in the *glass*; theories that consider this transition from the standpoint of the supercooled liquid are, in contrast, essentially theories of viscosity in which the glass transition marks the termination of the liquid regime.

To sum up, we note that the increase in amplitude of the transverse modes, $\langle x^2 \rangle$, at T_g seen in Mossbauer experiments is significant in that it suggests the possibility of developing an entirely new approach to the problem of the glass transition itself.

4. Computer simulation and particle motion

At the outset we note that computer simulation studies reported in the literature to date have concentrated upon elucidating particle motions in the neighbourhood of the glass transition (Frenkel and McTague 1980; Angell *et al* 1981). There appears to have been no study that has sought to describe either the TLS or, indeed, the other types of particle motion in the glassy state described earlier. However, computer simulation studies in supercooled regions which have been performed with realistic potentials have brought out some of the most significant features related to the glassy state. Both Monte Carlo (MC) (Raveche 1976; Raveche and Streett 1976; Wendt and Abraham 1978; Abraham 1980) and molecular dynamics (MD) (Kristensen 1976; Rahman *et al* 1976; McTague *et al* 1978; Clarke 1979) techniques may, in principle, be employed but the latter is preferred in studies of dynamic properties since it is the more direct approach to the

autocorrelation effects. In this section we summarize some of the recent computer simulation studies which, in our opinion, enable us to understand particle motion in the glass transition at a fundamental level.

In a recent article, Angell *et al* (1981) have reviewed computer simulation experiments to explore the effect of the (assumed) inter-particle potential upon glass formation. It is now well-known that computer simulation studies entail the use of very high rates of quenching ($\approx 10^{12}$ deg K sec^{-1}) (Angell 1982) and of a number of particles that usually does not exceed a few thousands (≈ 4000) (Cape and Woodcock 1979). Consequently, several features of the simulated glass transition do not completely match those of a 'real' glass transition. In these studies, the T_g itself is located through the behaviour of the diffusion coefficient (Angell *et al* 1981). In simple fluids, it has been found that diffusivity approaches zero at T_g more rapidly than is the case with related laboratory glasses. Further, diffusivity in a real glass can be quite low (10^{-18} cm^2 sec^{-1}) but in a simulated glass it is often more than 10^{-5} cm^2 sec^{-1}. This can be simply understood from the fact that in many simple polar molecules the product of $\tau_D D$ is a constant ($\approx 2 \times 10^{-16}$ cm^2) which for a diffusivity of 10^{-18} cm^2 sec^{-1} would give rise to relaxation times of ≈ 100 sec, the time-scale of laboratory experimental measurement. In the case of a simulated glass T_g would occur even at a diffusivity of roughly 10^{-6} cm^2 sec^{-1}, because the corresponding relaxation time would be $\approx 10^{-10}$ sec which is still roughly 100 times the simulated cooling rate. In such a short time the system can only relax vibrationally and not configurationally. It has also been noted (Damgaard-Kristensen 1976) that a simulated glass transition is rather smeared-out and that the density of a simulated glass is $\approx 7\%$ lower than that of comparable laboratory time-scale glasses. A more disturbing feature of these studies is the size dependence of the approach to equilibrium (Clarke 1979) which hints at the possibility that most reported measurements may not correspond to well-relaxed systems. The significant results of simulation studies are as follows. (a) They affirm that glass formation can, indeed, ensue from supercooling of the melt. (b) Glass formation appears to be controlled by the repulsive part of the potential: the softer the potential, the lower is the glass-forming tendency (Alder and Wainright 1960; Raveche 1976; Hoover *et al* 1971; Hiwatari 1978). This finding seems to accord very well with the fact that the alkali metals, which are described by soft potentials have, as yet, not been vitrified, in contrast to transition metals which have harder potentials and have been vitrified (Chen 1980). (d) Relaxational behaviour also appears to be controlled by the softness of the potential (Clarke 1979; Woodcock 1976, 1978; Barker *et al* 1975). Different types of potentials have been used in several reported studies and interesting results with respect to the structure of glasses so formed have been obtained. From the foregoing it is quite clear that the choice of an interaction potential has a profound influence both on the local structures in the simulated glasses and upon their relaxational behaviour.

5. Concluding remarks

In the foregoing sections we have discussed several approaches to the study of particle motions in glass that principally involve spectroscopic techniques. Other methods are indeed available: for instance, neutron scattering, that has been used with particular success in studies of motion in polymers, but we have not dealt either with this or with others such as x-ray and light scattering, hypersound propagation and diffusion

studies. Our choice has been directed by considerations of relevance of the technique to a large variety of glasses and of directness of the information obtained. We feel that the techniques discussed above meet such criteria to a greater extent than others, though it is debatable.

In the discussion of dielectric and mechanical relaxations, we have found that both variable temperature and variable frequency approaches have been used, wherein power absorbed from the imposed field is used for particle motion. Information in these techniques may consequently be directly related to jump frequencies and associated relaxation times. In resonance spectroscopy, on the other hand, information with respect to particle motion can be obtained only through perturbations caused to the absorption or emission band characteristics. These spectroscopic techniques are, nonetheless elegant, the mathematical apparatus available for data-analysis is powerful and data may be obtained about the particles whose motion is being studied. However, these techniques, particularly vibrational spectroscopy, are comparatively under-utilised in the context of the study of particle motion in glasses.

We may note that there are three generally distinct temperature regimes where different kinds of motion may be discussed, and each region is roughly determined by the thermal energy of the system. Motion at extremely low temperatures ($< 0{\cdot}2T_g$) is almost entirely localised and occurs between a pair of asymmetric, split-potential wells. Activation energies for such motion are low ($\approx$ 0·1 eV) and motion manifests itself in a host of low-temperature anomalies. There is now a large and growing body of evidence to show that such split-potential wells (TLS) are a typical feature of the glassy state. In network glasses TLS may be visualised as involving motion in the network but in molecular or discrete ion glasses these may involve small changes in orientation or position of ions within their cages. Between 0·2 and 0·8 T_g, both short range and long range motions begin to evolve within the glass. The strength of the absorption tends to be very low in lower temperature limits of this regime because of inherent broadening mechanisms. In this range of temperature activation barriers to motion range from 0·2 to 0·8 eV and the motion itself ranges from group motion to long range hopping of ions. Dielectric and mechanical relaxations at higher temperatures in this range are called β-relaxations and many systems with diverse types of bonding appear to exhibit this phenomenon. Alkali ion motion in a variety of glasses also appears in this temperature range. Mixed ion effects, in particular, seem to display characteristic behaviour in dielectric and other studies. Beyond 0·8 T_g, large scale particle motions begin to take place and separation of the various contributions is very difficult. Collective and cooperative movements that begin to appear in this region have still not been well understood even though Mossbauer experiments have provided significant information related to such motions.

Motion between 0·2 T_g and T_g strongly suggest the relevance of a cluster model, the basic ingredient of which is the existence of density fluctuations on a scale accessible to high resolution electron microscopy and small angle radiation or particle scattering. While experimental support for this model has been accumulating, modelling and analysis of particle motion remain to be carried out. It would be profitable to assume the presence of both density and composition fluctuations on a scale that does not cause macroscopic phase separation. We have already pointed out that motion, particularly of ions involved in electrical conductivity, may be traced to motion either in the tissue region or on cluster surfaces.

Particle motion studies as related to the nature of bonding have been inferred only

from simulation studies on liquids that, unfortunately, do not tell much about behaviour in the glass. However, the importance of repulsive potentials on glass formation may be extended to discern patterns of particle motion. Such patterns may well be grouped on the basis of the softness of the repulsive potential and a study along these lines should be particularly useful in understanding particle motion in fast ion conducting glasses.

Acknowledgement

The authors are grateful to Prof. C N R Rao for his kind encouragement.

References

Abraham F F 1980 *J. Chem. Phys.* **72** 359
Abras A and Mullen J G 1972 *Phys. Rev.* **A6** 2343
Alder B S and Wainright T E 1960 *J. Chem. Phys.* **33** 1439
Anderson O L and Bommel H F 1955 *J. Amer. Ceram. Soc.* **38** 125
Anderson P W, Halperin B I and Varma C M 1972 *Philos. Mag.* **25** 1
Angell C A 1980 in *Vibrational spectroscopy of molecular liquids and solids* (eds) S Bratos and R M Pick (NATO Advanced Study Institutes Series) Series B, Physics (New York: Plenum Press) Vol 56
Angell C A 1981 in *Preparation and characterization of materials* (eds) J M Honig and C N R Rao (New York: Academic Press)
Angell C A, Clarke J H R and Woodcock L V 1981 *Adv. Chem. Phys.* **48** 397
Angell C A and Rao K J 1972 *J. Chem. Phys.* **57** 4711
Antsiferova L I, Korst N N, Stryukov V B, Ivanova A N, Nazemets N S and Rabin'kina N V 1973 *Molec. Phys.* **25** 909
Arnold W, Hunklinger S, Stein S and Dransfeld K 1974 *J. Non-Cryst. Solids* **14** 192
Atake T and Angell C A 1980 *J. Non-Cryst. Solids* **38** and **39** 439
Ayscough P B 1967 *Electron spin resonance in chemistry* (London: Methuen)
Bailey R T 1974 in *Molecular spectroscopy* (eds) R F Barrow, D A Long and D J Millen (London: Chemical Society) p. 173
Ballaro S, Cubiotti G, Cutroni M, Frassica S and Wanderlingh F 1975 Il. *Nuovo Cimento* **B25** 13
Barker J A, Hoare M R and Finney J L 1975 *Nature (London)* **257** 120
Barlow A J, Lamb J and Matheson A J 1966 *Proc. R. Soc.* **262** 322
Barnes H and Langevin M 1963 *J. Phys.* **24** 1034
Bartholomew R F 1973 *J. Non-Cryst. Solids* **12** 321
Bartoli F J and Litovitz T A 1972 *J. Chem. Phys.* **56** 404, 413
Bloch F 1946 *Phys. Rev.* **70** 460
Bloembergen P, Purcell E M and Pound R V 1948 *Phys. Rev.* **73** 679
Boehm L, Ingram M D and Angell C A 1981 *J. Non-Cryst. Solids* **44** 305
Bondi A 1968 *Physical properties of molecular crystals, liquids and glasses* (New York: John Wiley and Sons)
Born M and Huang K 1954 *Dynamical theory of crystal lattices* (Oxford: Clarendon Press)
Bratos S and Maréchal E 1971 *Phys. Rev.* **A4** 1078
Brunot B, Hauser U and Neuwirth N 1971a *Z. Phys.* **249** 134
Brunot B, Hauser U, Neuwirth N and Bolz J 1971b *Z. Phys.* **249** 125
Bursill L A, Thomas J M and Rao K J 1981 *Nature (London)* **289** 157
Cahn R W 1980 *Contemp. Phys.* **21** 43
Cape J N and Woodcock L V 1979 *J. Chem. Phys.* **72** 976
Caporali R V 1964 *J. Am. Ceram. Soc.* **47** 412
Carini Jr G, Cutroni M, Galli G and Wanderlingh F 1978 *J. Non-Cryst. Solids* **30** 61
Carrington A and McLachlan A D 1967 *Introduction to magnetic resonance* (New York: Harper and Row)
Champeney D C 1979 *Rep. Prog. Phys.* **42** 1017
Charles R J 1965 *J. Amer. Ceram. Soc.* **48** 432
Chen H S 1980 *Rep. Prog. Phys.* **43** 353
Clarke J H R 1979 *J. Chem. Soc. Faraday Trans.* 2 **75** 1371

Clarke J H R and Miller S 1972 *Chem. Phys. Lett.* **13** 97
Cohen M H and Grest G S 1980 *Phys. Rev.* **B20** 1077
Cohen M H and Grest G S 1981 *Solid. State Commun.* **39** 143
Cole K S and Cole R H 1941 *J. Chem. Phys.* **9** 341
Cooper A R 1977 in *Physics of non-crystalline solids* (ed.) G H Frischat (Aedermannsdorf, Switzerland: Trans. Tech. Publications)
Damgaard-Kristensen W 1976 *J. Non-Cryst. Solids* **21** 303
Daniel V V 1967 *Dielectric relaxation* (London and New York: Academic Press)
Davidson D W and Cole R H 1951 *J. Chem. Phys.* **19** 1484
Davies R O and Jones G O 1953 *Adv. Phys.* **2** 370
Day D E 1974 *Relaxation processes in glasses* (ed.) D E Day (Amsterdam: North-Holland Publishing Company)
Debye P 1929 *Polar molecules* (New York: Reinhold)
Dekker A J 1967 *Solid state physics* (London: Macmillan) pp. 154–157
Doge G, Arndt R and Khuen A 1977 *Chem. Phys.* **21** 53
Doolittle A K 1951 *J. Appl. Phys.* **22** 1471
Douglas R W 1963 *Phys. Chem. Glasses* **4** 34
El-Bayoumi O H and MacCrone R K 1976 *J. Amer. Ceram. Soc.* **59** 386
Farley J M and Saunders G A 1975 *J. Non-Cryst. Solids* **18** 417
Fislia R A, Brodale G E, Hornung E W and Giauque W F 1969 *Rev. Sci. Instrum.* **40** 365
Fitzgerald J V 1951 *J. Amer. Ceram. Soc.* **34** 314
Fleming J W and Day D E 1972 *J. Amer. Ceram. Soc.* **55** 186
Flinn P A, Zabransky B J and Ruby S L 1976 *J. Phys. C6* **37** 739
Forry K E 1957 *J. Amer. Ceram. Soc.* **40** 90
Frenkel D and McTague J P 1980 *Ann. Rev. Phys. Chem.* **31** 491
Fulcher G S 1925 *J. Amer. Ceram. Soc.* **8** 339
Fuoss R M and Kirkwood J G 1941 *J. Amer. Chem. Soc.* **63** 385
Frohlich H 1958 *Theory of dielectrics* (London: Oxford University Press)
Gaskell P H, Smith D J, Catto C J D and Cleaver J R A 1979 *Nature (London)* **281** 465
Golding B, Graebner J E, Halperin B I and Schutz R J 1973 *Phys. Rev. Lett.* **30** 223
Goldstein M 1969 *J. Chem. Phys.* **51** 3728
Goldstein M 1975 *J. Phys. Paris Colloq.* **C2 C2-3**
Gordon R J 1965 *J. Chem. Phys.* **43** 1307
Gordon R J 1966 *J. Chem. Phys.* **44** 1830
Gordon R J 1968 *Adv. Mag. Res.* **3** 1
Gosselin J P, Shimony U, Grodzins L and Cooper A R 1968 *Phys. Chem. Glasses* **8** 56
Gupta P K and Moynihan C T 1976 *J. Chem. Phys.* **65** 4136
Gupta P K and Moynihan C T 1978 *J. Non-Cryst. Solids* **29** 143
Grant F A 1958 *J. Appl. Phys.* **29** 76
Gutowsky H S and McGarvey B R 1952 *J. Chem. Phys.* **20** 1472
Gutowsky H S and Pake G E 1950 *J. Chem. Phys.* **18** 162
Haddad J and Goldstein M 1978 *J. Non-Cryst. Solids* **30** 1
Hagy H E and Ritland H N 1957 *J. Amer. Ceram. Soc.* **40** 436
Hakim R M and Uhlmann D R 1971 *Phys. Chem. Glasses* **12** 132
Haven Y and Stevels J M 1956 *Proc. 4th Int. Cong. Glass* (Paris: Imprimerie Chaix) p. 343
Hayler L and Goldstein M 1977 *J. Chem. Phys.* **66** 4736
Hendrickson J R and Bray P J 1972a *Phys. Chem. Glasses* **13** 43
Hendrickson J R and Bray P J 1972b *Phys. Chem. Glasses* **13** 107
Hendrickson J R and Bray P J 1973 *J. Mag. Res.* **9** 341
Hendrickson J R and Bray P J 1974 *J. Chem. Phys.* **61** 2754
Higgins T J, Macedo P B and Volterra V 1972 *J. Amer. Ceram. Soc.* **55** 488
Hiwatari Y 1978 *Prog. Theor. Phys.* **59** 1401
Hoover W G, Gray S G and Johnson K W 1971 *J. Chem. Phys.* **55** 1128
Hunklinger S, Arnold W, Stein S, Nava R and Dransfeld K 1972 *Phys. Lett.* **A42** 253
Isard J O 1969 *J. Non-Cryst. Solids* **1** 235
Ivanov A O 1964 *Soc. Phys. Solid State* **5** 1933
Jagdt R 1960 *Glastech. Ber.* **33** 10

Johari G P and Goldstein M 1970 *J. Chem. Phys.* **53** 2372
Johari G P and Goldstein M 1971 *J. Chem. Phys.* **55** 4245
Kauzmann W 1942 *Rev. Mod. Phys.* **14** 12
Kauzmann W 1948 *Chem. Rev.* **43** 219
Kielson D and McClung R E D 1968 *J. Chem. Phys.* **49** 3380
Kostanyan K A 1960 *Structure of glass* Vol 2 (New York: Consultants Bureau) pp. 234–236
Kovac J 1981 *J. Phys. Chem.* **85** 2060
Kristensen W D 1976 *J. Non-Cryst. Solids* **21** 303
Kronig R deL 1939 *Physica* **6** 33
Kurkjian C R and Krause J T 1968 *J. Amer. Ceram. Soc.* **51** 226
Lakatos A I and Abkowitz M 1971 *Phys. Rev.* **B3** 1791
Lascombe J 1974 See the articles in *Particle motion in liquids* (ed.) J Lascombe (Dordrecht, Holland: D. Reidel Publishing Company)
Lidiard A B 1957 in *Handbuch der physik* Vol 20 (Berlin: Springer-Verlag) p. 275
Litovitz T A and Davis C M 1965 in *Physical acoustics* (ed.) W P Mason (New York: Academic Press)
Lovell M C, Avery A J and Vernon M W 1976 *Physical properties of materials* (London: van Nostrand Remhold Company)
Macedo P B, Moynihan C T and Bose R 1972 *Phys. Chem. Glasses* **13** 171
Macedo P B and Napolitano A 1967 *J. Res. NBS* **A71** 231
Mahle S H and McCammon R D 1969 *Phys. Chem. Glasses* **6** 222
Mansingh A, Dhawan A, Tandon R P and Vaid J K 1978 *J. Non-Cryst. Solids* **27** 309
Mansingh A, Reyes J M and Sayer M 1972 *J. Non-Cryst. Solids* **7** 12
Mansingh A, Tandon R P and Vaid J K 1975 *J. Phys. Chem. Solids* **36** 1267
Mansingh A, Vaid J K and Tandon R P 1976 *J. Phys.* **C9** 1809
Materials Advisory Board 1968 *Nat. Acad. Sci. Res. Council MAB*, Report 243
Maxwell J C 1954 *A treatise on electricity and magnetism* Vol 1 (Dover: Dover Publications) p. 452
McTague J P, Mandell M J and Rahman A 1978 *J. Chem. Phys.* **68** 1876
Mohyuddin J and Douglas R W 1960 *Phys. Chem. Glasses* **1** 70
Muller-Warmuth W and Otte W 1980 *J. Chem. Phys.* **72** 1749
Nafie L A and Peticolas W L 1972 *J. Chem. Phys.* **57** 3145
Namikawa H 1975 *J. Non-Cryst. Solids* **18** 173
Narayanaswamy O S 1971 *J. Amer. Ceram. Soc.* **54** 491
Ng D and Sladek R J 1975 *Phys. Rev.* **B11** 4017
Ohta H 1975 *Glass Tech.* **16** 25
Owen A E 1963 in *Progress in ceramic science* (ed.) J E Burke (London: Pergamon Press)
Pake G E and Estle T L 1973 *The physical principles of electron paramagnetic resonance* (Reading, U.K.: Benjamin)
Parthasarathy R, Rao K J and Rao C N R 1981 *J. Phys. Chem.* **85** 3085
Parthasarathy R, Rao K J and Rao C N R 1982 *Chem. Phys.* **68** 393
Perez J, Duperray B and Lefevre D 1981 *J. Non-Cryst. Solids* **44** 113
Philippoff W 1965 in *Physical acoustics* (ed.) W P Mason (New York and London: Academic Press)
Phillips W A 1972 *J. Low Temp. Phys.* **7** 351
Poole C A and Farach H A 1971 *Relaxation in magnetic resonance* (New York: Academic Press)
Quinten H J C A, van Gemert W J Th and Stevels J M 1978 *J. Non-Cryst. Solids* **29** 333
Rahman A, Mandell M J and McTague J P 1976 *J. Chem. Phys.* **64** 1564
Rao C N R and Rao K J 1978 *Phase transitions in solids* (New York: McGraw-Hill)
Rao K J 1979 *Bull. Mater. Sci.* **1** 181
Rao K J 1980 *Bull. Mater. Sci.* **2** 357
Rao K J 1982 in *Preparation and characterization of materials* (eds) J M Honig and C N R Rao (New York: Academic Press)
Rao K J and Sundar H G K 1980 *Phys. Chem. Glasses* **21** 216
Ravache H J 1976 *Ann. N.Y. Acad. Sci.* **279** 36
Ravache H J and Streett W B 1976 *J. Res. NBS*, **A80** 59
Rawson H 1967 *Inorganic glass-forming systems* (London: Academic Press)
Raychaudari A K and Pohl R O 1981 *Solid State Commun.* **37** 105
Ritland H N 1954 *J. Amer. Ceram. Soc.* **37** 370
Rotger H 1941 *Glastech. Ber.* **19** 192

Rotger H 1958 *Glastech. Ber.* **31** 54
Rothschild J 1974 in *Molecular motions in liquids* (ed.) J Lascombe (Dordrecht, Holland: D. Reidel Publishing Company)
Rothschild W G 1976 *J. Chem. Phys.* **65** 455
Rubinstein M 1976 *Phys. Rev.* **B14** 2778
Rubinstein M and Resing H A 1976 *Phys. Rev.* **B13** 459
Ruby S L, Love J C, Flinn P A and Zabransky B J 1975 *Appl. Phys. Lett.* **27** 320
Ruby S L, Zabransky B J and Flinn P A 1976 *J. Phys. C*6, **37**, 745
Ryder R J and Rindone G E 1960 *J. Amer. Ceram. Soc.* **43** 662
Ryder R J and Rindone G E 1961 *J. Amer. Ceram. Soc.* **44** 532
Sakurai J and Ooka K 1968 *Toshiba Rev.* **23** 913
Schumacher R T 1970 *Introduction to magnetic resonance* (New York: Benjamin)
Shelby J E and Day D E 1969 *J. Amer. Ceram. Soc.* **52** 169
Shelby J E and Day D E 1970 *J. Amer. Ceram. Soc.* **53** 18
Simopoulos A, Wickman H, Kostikas A and Petrides D 1970 *Chem. Phys. Lett.* 7 615
Stevels J M 1951 *Verres. Refract.* **5** 4
Stevels J M 1957 in *Handbuch der physik* Vol 20 (Berlin: Springer-Verlag) p. 350
Stevels J M 1977 in *The physics of non-crystalline solids* (ed.) G H Frischat (Aedermannsdorf, Switzerland: Trans. Tech. Publications)
Stevels J M 1980 *J. Non-Cryst. Solids* **40** 69
Stone T J, Buckman T, Nordis F L and McConnell H M 1965 *Proc. Natl. Acad. Sci. (USA)* **54** 1010
Sundar H G K, Parthasarathy R and Rao K J 1982 *Z. Naturforsch.* **A37** 191
Sundar H G K and Rao K J 1982a *Proc. Indian Acad. Sci.* **91** 207
Sundar H G K and Rao K J 1982b *Pramana* **19** 125
Szeftel J and Alloul H 1978 *J. Non-Cryst. Solids* **29** 253
Tammann G and Hesse W 1926 *Z. Anorg. Allgen. Chem.* **156** 245
Taylor H E 1956 *Trans. Far. Soc.* **52** 873
Taylor H E 1959 *J. Soc. Glass Tech.* **43** 124T
Terai R 1971 *J. Non-Cryst. Solids* **6** 121
Terai R and Hayami R 1975 *J. Non-Cryst. Solids* **18** 217
Thurzo I 1975 *J. Non-Cryst. Solids* **18** 129
Tyagi S and Lord A E 1979 *J. Non-Cryst. Solids* **30** 273
Urnes S 1967 *Phys. Chem. Glasses* **8** 125
van Ass H M and Stevels J M 1974a *J. Non-Cryst. Solids* **15** 215
van Ass H M and Stevels J M 1974b *J. Non-Cryst. Solids* **16** 46
van Gemert W J 1977 in *Physics of non-crystalline solids* (ed.) G H Frischat (Aedermannsdorf, Switzerland: Trans. Tech. Publications) p. 548
van Gemert W J, van Ass H M and Stevels J M 1974 *J. Non-Cryst. Solids* **16** 281
van Gemert W J and Stevels J M 1978 *J. Non-Cryst. Solids* **30** 135
van Konynenburg P and Steele W A 1975 *J. Chem. Phys.* **62** 2301
van Vleck J H 1939 *J. Chem. Phys.* 7 72
Vasquez A and Flinn P A 1980 *J. Chem. Phys.* **72** 1958
Vogel H 1921 *Phys. Z.* **22** 645
Wagner K W 1913 *Ann. Phys.* **24** 711
Wagner K W 1914 *Arch. Elektrotech.* **2** 371
Wendt H R and Abraham F F 1978 *Phys. Rev. Lett.* **41** 1244
Wertheim G K 1964 *Mossbauer effect: Principles and applications* (New York: Academic Press)
Weyl W A and Marboe E C 1962 *The constitution of glasses* Vol II, Parts I and II, (New York: Interscience)
Williams E and Angell C A 1973 *J. Polym. Sci. Polym. Lett.* **11** 383
Wong J and Angell C A 1976 *Glass: Structure by spectroscopy* (New York: Marcel Dekker)
Woodcock L V 1976 *J. Chem. Soc. Faraday* 2 **72** 1667
Woodcock L V 1978 *J. Chem. Soc. Faraday* 2 **74** 11
Yarwood J and Arndt R 1979 in *Molecular association* Vol 2 (ed.) R Foster (New York: Wiley) Chap. 4
Young R P and Jones R N 1971 *Chem. Rev.* **71** 219
Zdaniewski W A, Rindone G E and Day D E 1979 *J. Mater. Sci.* **14** 763